NTIS # PB2004-101322

# SSC-431

# RETENTION OF WELD METAL PROPERTIES AND PREVENTION OF HYDROGEN CRACKING



SHIP STRUCTURE COMMITTEE
2003

# SHIP STRUCTURE COMMITTEE

RADM Thomas H. Gilmour
U. S. Coast Guard Assistant Commandant,
Marine Safety and Environmental Protection
Chairman, Ship Structure Committee

Mr. W. Thomas Packard
Director,
Survivability and Structural Integrity Group
Naval Sea Systems Command

Dr. Donald Liu
Senior Vice President
American Bureau of Shipping

Mr. Joseph Byrne
Director, Office of Ship Construction
Maritime Administration

Mr.Gerard A. McDonald
Director General, Marine Safety,
Safety & Security
Transport Canada

Mr. Thomas Connors
Director of Engineering
Military Sealift Command

Dr. Neil Pegg
Group Leader - Structural Mechanics
Defence Research & Development Canada - Atlantic

**CONTRACTING OFFICER TECHNICAL REP.**
Chao Lin / MARAD
Natale Nappi / NAVSEA
Robert Sedat / USCG

**EXECUTIVE DIRECTOR**
Lieutenant Eric M. Cooper
U. S. Coast Guard

## SHIP STRUCTURE SUB-COMMITTEE

**AMERICAN BUREAU OF SHIPPING**
Mr. Glenn Ashe
Mr. Yung Shin
Mr. Phil Rynn
Mr. William Hanzalek

**DEFENCE RESEARCH & DEVELOPMENT ATLANTIC**
Dr David Stredulinsky
Mr. John Porter

**MARITIME ADMINISTRATION**
Mr. Chao Lin
Mr. Carlos Setterstrom
Mr. Richard Sonnenschein

**MILITARY SEALIFT COMMAND**
Mr. Joseph Bohr
Mr. Rick A. Anderson
Mr. Michael W. Touma

**NAVAL SEA SYSTEMS COMMAND**
Mr. Jeffery E. Beach
Mr. Edward E. Kadala
Mr. Allen H. Engle
Mr. Charles L. Null

**TRANSPORT CANADA**
Mr. Jacek Dubiel

**UNITED STATES COAST GUARD**
Mr. Rubin Sheinberg
Mr. Robert Sedat
Commander Ray Petow

**CANADIAN COAST GUARD**
Mr. Daniel Gauvin

Member Agencies:

*American Bureau of Shipping*
*Defence Research Establishment Atlantic*
*Maritime Administration*
*Military Sealift Command*
*Naval Sea Systems Command*
*Society of Naval Architects & Marine Engineers*
*Transport Canada*
*United States Coast Guard*

Ship
Structure
Committee

Address Correspondence to:

Executive Director
Ship Structure Committee
U.S. Coast Guard (G-MSE/SSC)
2100 Second Street, SW
Washington, D.C. 20593-0001
Ph: (202) 267-0003
Email: ecooper@comdt.uscg.mil

**SSC – 431**
**SR – 1357**

**November 2003**

# RETENTION OF WELD METAL PROPERTIES AND PREVENTION OF HYDROGEN CRACKING

Single and multiple pass weldability tests were used to assess hydrogen-cracking resistance of weld metals used for joining conventional quenched and tempered HY-100 steel and a lower carbon HSLA-100 steel. A multiple pass weldability test based on a slotted cruciform specimen was developed and the results of the slotted cruciform test were compared to single pass weldability test results. Weld metal chemical composition, diffusible hydrogen content, and thermal history were variables investigated in this study. Additional studies included evaluation of weld metal hydrogen cracking resistance of lower strength HSLA-80 and HSLA-65 steels.

The results from this study indicate that it is possible to correlate diffusible hydrogen level and hardenability of the weld deposit to hydrogen cracking resistance. The single pass WIC test was useful in establishing cracking versus no cracking conditions. The slotted cruciform test was effective for comparing longitudinal versus transverse cracking tendencies. Welding conditions that resulted in hydrogen embrittlement were determined by evaluation of all weld metal tensile specimens removed from the cruciform specimen.

The result of this study was the development of a mathematical crack prediction model to correlate the weld metal chemical composition and diffusible hydrogen content with critical cooling time in order to avoid hydrogen cracking in single and multiple pass welds.

T. H. GILMOUR
Rear Admiral, U.S. Coast Guard
Chairman, Ship Structure Committee

**Technical Report Documentation Page**

| 1. Report No.<br>SSC-431 | 2. Government Accession No.<br>**PB2004-101322** | 3. Recipient's Catalog No.<br>SR-1357 |
|---|---|---|
| 4. Title and Subtitle<br><br>RETENTION OF WELD METAL PROPERTIES AND PREVENTION OF HYDROGEN CRACKING | | 5. Report Date<br>December 2003<br>6. Performing Organization Code |
| 7. Author(s)<br><br>R.J. Wong | | 8. Performing Organization Report No.<br>NSWCCD-61-TR-2003/03 |
| 9. Performing Organization Name and Address<br>Naval Suface Warfare Center Carderock Division<br>West Bethesda, MD 20817-5700 | | 10. Work Unit No. (TRAIS)<br>11. Contract or Grant No. |
| 12. Sponsoring Agency Name and Address<br>Ship Structure Committee<br>C/O Commandant (G-MSE/SSC)<br>United States Coast Guard<br>2100 Second Street, SW<br>Washington, DC 20593-0001 | | 13. Type of Report<br>Final Report<br>14. Sponsoring Agency Code<br>**G-M** |
| 15. Supplementary Notes<br>Sponsored by the Ship Structure Committee and its member agencies | | |


**16. Abstract**

In this project, single and multiple pass weldability tests were used to assess hydrogen-cracking resistance of weld metals used for joining conventional quenched and tempered HY-100 steel and a lower carbon HSLA-100 steel. Additional studies included evaluation of weld metal hydrogen cracking resistance of lower strength HSLA-80 and HSLA-65 steels. The Welding Institute of Canada (WIC) restraint-cracking test was used as the single pass weldability test. A slotted cruciform specimen was used as the multiple pass weldability test. Weld metal chemical composition, diffusible hydrogen content, and thermal history were variables investigated in this study. The filler materials included electrodes typically used for welding 552 and 690 MPa (80 and 100 ksi) yield strength steels.

The results from this study indicate that it is possible to correlate diffusible hydrogen level and hardenability of the weld deposit to hydrogen cracking resistance. The single pass test was useful in establishing cracking versus no cracking conditions. The slotted cruciform test was effective for comparing longitudinal versus transverse cracking tendencies. Welding conditions that resulted in hydrogen embrittlement were determined by evaluation of all weld metal tensile specimens removed from the cruciform specimen.

The result of this study was the development a mathematical crack prediction model to correlate the weld metal chemical composition and diffusible hydrogen content with critical cooling time in order to avoid hydrogen cracking in single and multiple pass welds.


| 17. Key Words | 18. Distribution Available From:<br>National Technical Information Service<br>U.S. Department of Commerce<br>Springfield, VA 22151<br>Ph. (703) 605-6000 | | |
|---|---|---|---|
| 19. Security Classif. (of this report)<br>**Unclassified** | 20. Security Classif. (of this page)<br>**Unclassified** | 21. No. of Pages<br>**58** | 22. Price<br>PC - $32 (A05)<br>ED - $9 (A00) |

**CONVERSION FACTORS**
**(Approximate conversions to metric measures)**

| To convert from | to | Function | Value |
|---|---|---|---|
| **LENGTH** | | | |
| inches | meters | divide | 39.3701 |
| inches | millimeters | multiply by | 25.4000 |
| feet | meters | divide by | 3.2808 |
| **VOLUME** | | | |
| cubic feet | cubic meters | divide by | 35.3149 |
| cubic inches | cubic meters | divide by | 61,024 |
| **SECTION MODULUS** | | | |
| $inches^2$ $feet^2$ | $centimeters^2$ $meters^2$ | multiply by | 1.9665 |
| $inches^2$ $feet^2$ | $centimeters^3$ | multiply by | 196.6448 |
| $inches^4$ | $centimeters^3$ | multiply by | 16.3871 |
| **MOMENT OF INERTIA** | | | |
| $inches^2$ $feet^2$ | $centimeters^2$ meters | divide by | 1.6684 |
| $inches^2$ $feet^2$ | $centimeters^4$ | multiply by | 5993.73 |
| $inches^4$ | $centimeters^4$ | multiply by | 41.623 |
| **FORCE OR MASS** | | | |
| long tons | tonne | multiply by | 1.0160 |
| long tons | kilograms | multiply by | 1016.047 |
| pounds | tonnes | divide by | 2204.62 |
| pounds | kilograms | divide by | 2.2046 |
| pounds | Newtons | multiply by | 4.4482 |
| **PRESSURE OR STRESS** | | | |
| $pounds/inch^2$ | $Newtons/meter^2$ (Pascals) | multiply by | 6894.757 |
| kilo $pounds/inch^2$ | mega $Newtons/meter^2$ (mega Pascals) | multiply by | 6.8947 |
| **BENDING OR TORQUE** | | | |
| foot tons | meter tons | divide by | 3.2291 |
| foot pounds | kilogram meters | divide by | 7.23285 |
| foot pounds | Newton meters | multiply by | 1.35582 |
| **ENERGY** | | | |
| foot pounds | Joules | multiply by | 1.355826 |
| **STRESS INTENSITY** | | | |
| kilo $pound/inch^2$ $inch^{1/2}$ ($ksi\sqrt{in}$) | mega Newton $MNm^{3/2}$ | multiply by | 1.0998 |
| **J-INTEGRAL** | | | |
| kilo pound/inch | $Joules/mm^2$ | multiply by | 0.1753 |
| kilo pound/inch | kilo $Joules/m^2$ | multiply by | 175.3 |

**CONTENTS**

Page

## FIGURES

**Page**

**TABLES**

**Page**



## Abbreviations

| | |
|---|---|
| AWM | all weld metal |
| CEN | carbon-equivalent number |
| GMAW | gas metal-arc welding |
| HAZ | heat affected zone |
| Hd | diffusible hydrogen |
| HSLA | high strength low alloy (followed by minimum yield strength in ksi) |
| HY | high yield strength (followed by minimum yield strength in ksi) |
| Pcm | composition characterizing parameter |
| SMAW | shielded metal-arc welding |
| $t_{100}$ | time to cool to 100 º C |
| WIC | Welding Institute of Canada |

## ABSTRACT

In this study, single and multiple pass weldability tests were used to assess hydrogen-cracking resistance of weld metals used for joining conventional quenched and tempered HY-100 steel and a lower carbon HSLA-100 steel. Additional studies included evaluation of weld metal hydrogen cracking resistance of lower strength HSLA-80 and HSLA-65 steels. The Welding Institute of Canada (WIC) restraint-cracking test was used as the single pass weldability test. A slotted cruciform specimen was used as the multiple pass weldability test. Weld metal chemical composition, diffusible hydrogen content, and thermal history were variables investigated in this study. The filler materials included electrodes typically used for welding 552 and 690 MPa (80 and 100 ksi) yield strength steels.

The results from this study indicate that it is possible to correlate diffusible hydrogen level and hardenability of the weld deposit to hydrogen cracking resistance. The single pass WIC test was useful in establishing cracking versus no cracking conditions. The slotted cruciform test was effective for comparing longitudinal versus transverse cracking tendencies. Welding conditions that resulted in hydrogen embrittlement were determined by evaluation of all weld metal tensile specimens removed from the cruciform specimen.

The result of this study was the development a mathematical crack prediction model to correlate the weld metal chemical composition and diffusible hydrogen content with critical cooling time in order to avoid hydrogen cracking in single and multiple pass welds.

## ADMINISTRATIVE INFORMATION

This report was prepared with the support of the Ship Structure Committee under task 1357, and the Office of Naval Research 6.2 Seaborne Materials Program. The report was prepared under the supervision of Mr. J. DeLoach, Welding & NDE Branch, Naval Surface Warfare Center, Carderock Division (NSWCCD 615).

## EXECUTIVE SUMMARY

### Scope

This program investigated the weldability of high strength steels, with emphasis on the hydrogen cracking resistance of the welding consumables used for joining them. A multiple pass weldability test based on a slotted cruciform specimen was developed. The results of the slotted cruciform test were compared to single pass weldability test results. A weld metal cracking versus no cracking response surface was developed to identify the critical cooling times to 100 °C ($t_{100critical}$) for different combinations of diffusible hydrogen and chemistry that are necessary to avoid weld metal hydrogen cracking.

Initial studies focused on relative high strength MIL-100S and MIL-120S type gas metal arc welding consumables that have been used for joining 690 MPa (100 ksi) yield strength HSLA-100 and HY-100 steels. Additional studies included evaluation of the hydrogen cracking resistance of HSLA-100 and HY-100 welded using higher strength MIL-14018-M electrodes as well as evaluation of lower strength leaner chemistry MIL-70S type consumables, which can be used for joining 552 MPa (80 ksi) HSLA-80 and 448 MPa (65 ksi) HSLA-65 steels.

**Thermal Severity**

The effect of using different weldability tests and plate thickness on thermal severity was investigated. Two thermal severity parameters were considered. The first was weld metal cooling rate at 573 °C (1000° F). The cooling rate at 573 °C affects the final microstructure and mechanical properties. The second parameter evaluated was the weld metal cooling time to 100 °C ($t_{100}$). This parameter is determined by measuring the time from extinguishing the arc until the weld metal surface has reached 100 °C. $T_{100}$ is an indirect measure of how easily hydrogen can diffuse out of the weld, with longer cooling times allowing more hydrogen to diffuse out of the weld. The multiple pass slotted cruciform specimen generally provided higher cooling rates at 573 °C and lower $t_{100}$ values compared to the single pass Welding Institute of Canada (WIC) type specimen.

**Metallography and hardness**

Metallography was performed to evaluate the extent and location of hydrogen cracks. Rockwell C hardness measurements were performed on macrosections removed from the cruciform specimens. The hardness values were correlated to the Pcm and CEN carbon equivalent equations.

**Tensile Property Characterization**

All weld metal tensile specimens were removed from the HY-100 and HSLA-100 cruciform specimens and evaluated in the as-welded condition. Specimens from the MIL120S weld deposits that were fabricated with an ambient temperature preheat exhibited reduced ductility associated with hydrogen embrittlement. Post weld thermal soaking of the MIL-120S tensile specimens prior to testing eliminated the ductility loss, confirming this was a hydrogen embrittlement problem. Tensile tests on weld deposits fabricated under similar conditions using lower strength MIL-100S and MIL-70S consumables did not show signs of hydrogen embrittlement.

**Predictive Model**

A predictive model to estimate weld metal hydrogen cracking resistance was developed. The effect of the chemical composition on cracking and the effect of diffusible hydrogen content on cracking were independently evaluated. The effect of the above two independent variables was then combined to form a three-dimensional hydrogen cracking/no-cracking surface based on the weld metal chemical composition and diffusible hydrogen content. A parameter called "the critical cooling time to 100 °C" ($t_{100, critical}$) was used to described hydrogen cracking resistance.

## INTRODUCTION

**Hydrogen Cracking**

Cold cracking, hydrogen assisted cracking, delayed cracking, heat affected zone cracking, underbead cracking, and hydrogen embrittlement cracking are different terms used to describe the same phenomenon, hydrogen cracking. This is an insidious problem that may not manifest itself until several days after welding is completed. It is well known that high strength steel welds can experience hydrogen cracking if the following conditions are present: (1) a critical concentration of hydrogen in the weld; (2) a crack susceptible microstructure; (3) a temperature in the range between -100 °C and +200 °C; and, (4) a tensile stress exceeding a threshold value. Several mechanisms have been proposed to explain hydrogen cracking. These theories include the following:

1. Internal Pressure Theory. Hydrogen atoms diffuse through steel and accumulate at microscopic defects. The formation of molecular hydrogen results in high internal pressure at the defect. The combined effect of applied stress and internal pressure results in reduction of the apparent fracture stress, reference [1] (Note: references are listed on page 47).
2. Petch and Stables Model. Hydrogen is absorbed at the crack tip and causes a reduction in surface energy that must be overcome for crack extension, reference [2].
3. Triaxial Stress Theory. Hydrogen will diffuse to regions of high triaxial stress. When a critical level of hydrogen is present a microcrack occurs. Under constant load conditions the region ahead of the

crack tip is then under high triaxial stress and diffusion of hydrogen to this region occurs. This type of cyclic propagation continues, resulting in a macro-crack, reference [3].

4. Hydrogen Dislocation Interaction Model. The presence of hydrogen in the lattice structure may restrict dislocation motion, thereby contributing to lattice embrittlement, reference [4].

5. Dislocation Model Beachem proposed a theory that hydrogen in the lattice structure could increase both dislocation density and the generation of new dislocations. In this model crack tip plasticity is enhanced by the presence of hydrogen. The resulting plastic deformation promotes diffusion of hydrogen ahead of the crack tip, reference [5].

Despite different viewpoints on the exact mechanism for hydrogen cracking, all of these theories recognize that cracking is caused by a combination of hydrogen, a susceptible microstructure, and the presence of a tensile stress.

**Welding Requirements**

Historically, high strength carbon and low alloy steels have required some form of welding controls such as a minimum preheat temperature and/or post-weld heat treatment in order to avoid hydrogen related problems. The carbon content and other alloying content of many steels are high enough to promote the formation of hard microstructures in the heat-affected zone (HAZ) of the weldment during welding. Hard microstructures are often sensitive to hydrogen embrittlement and cracking problems. Several equations, nomographs, and algorithms have been developed in order to estimate safe welding conditions that prevent HAZ hydrogen cracking, references [6] and [7]. In many cases these equations, nomographs, and algorithms are based on the results of single-pass, laboratory-type HAZ weldability tests.

Advances in clean steel making and plate processing practices have led to the development of high strength steels with lower carbon and alloying additions. These high strength low alloy (HSLA) steels have been shown to be more weldable and resistant to heat affected zone hydrogen cracking problems than conventional quenched and tempered steels of comparable strength levels, references [8], [9] and [10].

Welding consumables developed for steels are normally designed to have a minimum weld metal yield strength that is greater than the base plate minimum yield strength, an overmatching strength weld.

This is done to "protect" the weld metals, which are prone to fabrication defects (porosity, slag, etc.) and to ensure that there is 100 percent joint efficiency during tensile loading of the weldment, reference [11]. As higher strength steels were developed, the need for an overmatching yield strength weld metal was re-evaluated. Several studies were performed that demonstrated that matching and slightly undermatching yield strength weld metals will provide satisfactory performance under a variety of loading conditions, references [12], [13] and [14].

Similarly, there have been improvements made in several of the welding consumables available today. These improvements include lower hydrogen electrodes that provide higher toughness weld metals. Use of more weldable base plate systems in conjunction with improved matching or undermatching strength welding consumables may permit relaxation in some costly fabrication restrictions, such as minimum preheat / maximum interpass temperatures, interlayer thermal soak treatments and post-weld thermal soak treatments. Therefore, the hydrogen cracking resistance of welding consumables used for welding of traditional and new high strength steels was investigated to determine whether current welding guidelines for preventing weld metal cracking, references [15] and [16] were still applicable and to provide the technical basis for establishing modified, potentially more cost effective guidelines.

## OBJECTIVE

The primary objective of this study was to characterize the hydrogen cracking resistance of high strength steel weld metals as a function of chemical composition and diffusible hydrogen (Hd) content. A second objective was to contrast the tendency for longitudinal versus transverse weld metal cracking in multipass welds. The final objective was to develop a predictive model for weld metal hydrogen cracking based on chemical composition and diffusible hydrogen level.

## APPROACH

The initial emphasis of this work focused on the weld metal hydrogen cracking resistance of weldments produced in 690 MPa (100 ksi) minimum yield strength steel plate (i.e., HY-100 and HSLA-

100) using matching and overmatching welding electrodes (i.e., MIL-120S and MIL-14018-M electrodes). Studies were also performed on HY-100 and HSLA-100 plate using undermatching strength MIL-100S electrodes. In addition, weldability tests were performed using lower yield strength plate and electrode materials to evaluate the effect of leaner chemistry on hydrogen cracking resistance. Single pass weldability tests were performed to characterize the effect of thermal history, chemistry, and diffusible hydrogen level on weld metal cracking resistance. Multi-pass weldability tests were also performed to contrast the propensity for longitudinal versus transverse weld metal cracking during multipass welding. The results of the multiple pass weldability tests were compared to the single pass weldability tests in order to determine if hydrogen cracking resistance of multipass welds can be predicted by single pass weldability tests. The results of these tests and analysis were used to develop a crack prediction model. Application of the hydrogen crack prediction model to determine whether preheat is required is schematically illustrated in Figure 1. (Note: abbreviations are presented on page v).

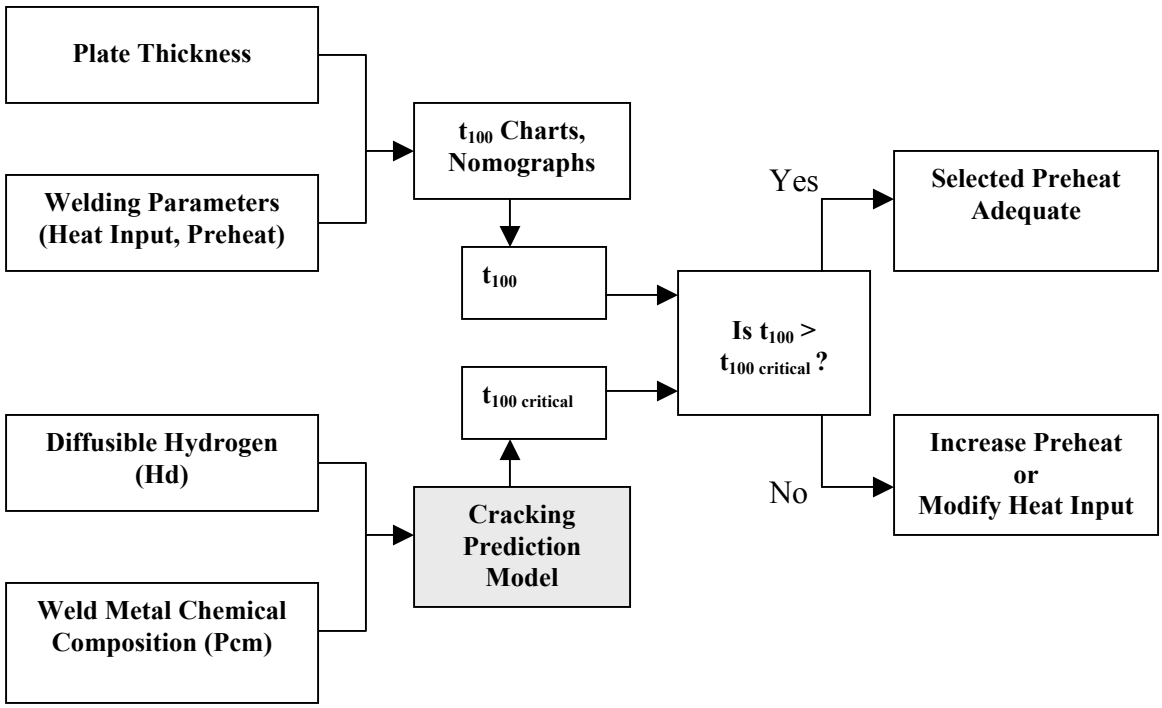


**Figure 1. Application of weld metal hydrogen cracking prediction model.**

## MATERIALS

The base materials employed in this investigation are listed in Table 1. The effects of changes in chemical composition on the likelihood of forming hard microstructures were assessed by calculation of carbon equivalent numbers.

Table 1. Chemical composition and carbon equivalents of the base plate materials

| | C | Mn | Si | Ni | Mo | Cr | Cu | Pcm [1] | CEN [2] |
|---|---|---|---|---|---|---|---|---|---|
| HY-100 | 0.153 | 0.25 | 0.20 | 2.60 | 0.26 | 1.26 | 0.12 | 0.30 | 0.60 |
| HSLA 100[3] | 0.037 | 0.78 | 0.27 | 3.17 | 0.62 | 0.56 | 1.36 | 0.29 | 0.38 |
| HSLA 100[4] | 0.056 | 0.76 | 0.23 | 3.41 | 0.59 | 0.63 | 1.51 | 0.31 | 0.41 |
| HSLA-80 | 0.06 | 0.6 | 0.30 | 0.87 | 0.22 | 0.75 | 1.15 | 0.26 | 0.36 |
| HSLA-65 | 0.08 | 1.39 | 0.22 | 0.35 | 0.06 | 0.16 | 0.25 | 0.19 | 0.28 |

1. Pcm is the Ito and Bessyo carbon equivalent equation, reference [17]
2. CEN is a Yurioka's carbon equivalent equation, reference [18]
3. 19 mm thick plate used in WIC tests
4. 25 mm thick plate used in cruciform tests

Ito and Bessyo's Pcm equation, reference [17] given in equation (1) and Yurioka's carbon equivalent number (CEN), references [18] and [19] given in equation (2) are the two carbon equivalent equations used in this study. The welding consumables used in this investigation are listed in Table 2.

Equation (1) $$Pcm = C + Si/30 + (Mn+Cr+Cu)/20 + Ni/60 + Mo/15 + V/10 + 5B$$

Equation (2) $$CEN = C + A(c) \times [Si/24 + Mn/6 + Ni/20 + (Cr+Mo+Nb+V)/5 + 5B]$$

where $$A(c) = 0.75 + 0.25 \times \tanh[20 \times (C-0.12)]$$

Table 2. Chemical composition of welding consumables

| | C | Mn | Si | Ni | Mo | Cr | Cu | Pcm [1] | CEN [2] |
|---|---|---|---|---|---|---|---|---|---|
| MIL-14018 [3] | 0.11 | 0.88 | 0.30 | 3.75 | 0.86 | 1.05 | 0.075 | 0.37 | 0.64 |
| MIL-120S | 0.07 | 2.03 | 0.40 | 2.58 | 0.55 | 0.38 | 0.02 | 0.29 | 0.45 |
| MIL-100S | 0.06 | 1.72 | 0.32 | 1.86 | 0.33 | 0.09 | 0.01 | 0.22 | 0.32 |
| MIL-70S | 0.10 | 1.4 | 0.82 | ---- | ---- | ---- | 0.04 | 0.19 | 0.28 |

1. Pcm is the Ito and Bessyo carbon equivalent equation, reference [17].
2. CEN is a Yurioka's carbon equivalent equation, reference [18]
3. Determined from deposited weld metal, other values determined from analysis of wire.

## EXPERIMENTAL PROCEDURES

### Welding Procedure

The gas metal-arc welding (GMAW) process in the spray mode was the primary welding process used in this investigation. GMAW was performed using a 95 percent Ar, 5 percent $CO_2$ shielding gas mixture. Some shielding gas was purchased with hydrogen premixed in the bottle. This was done to increase the diffusible hydrogen in selected weldability tests. Nominal GMAW parameters were 30 volts, 380 amps, and a welding travel speed of 7 mm/sec. These welding parameters resulted in a heat input of 1.6 kJ/mm. Shielded metal arc welding (SMAW) using a MIL-14018 electrode was also evaluated in this study. Nominal SMAW parameters were 24 volts, 150 amps and travel speed of 2.2 mm/s. The SMAW parameters also resulted in a heat input of 1.6 kJ/mm. All welding was performed in the flat position. Most of the weldability tests were performed at ambient temperature (17°C to 23°C) without added preheat. Some weldability specimens were preheated to modify thermal severity.

The weld metal cooling rate at 573 °C was measured using a thermocouple plunge. The time to cool to 100 °C , ($t_{100}$), was determined by measuring the time from extinguishing the arc to that when the surface temperature of the weld metal reached 100 °C.

### Single Pass Weldability Tests

The WIC test, reference [20], was used to characterize the effect of chemical composition and diffusible hydrogen level on weld metal hydrogen cracking resistance in single pass welds. WIC tests were performed using both HY-100 and HSLA-100 plate and MIL-100S, MIL-120S and MIL-14018 welding electrodes. The WIC specimen is illustrated in Figure 2 .The two halves of the WIC specimen

are fillet welded to either a two-inch thick plate or a one-inch thick tee stiffener plate to provide restraint.

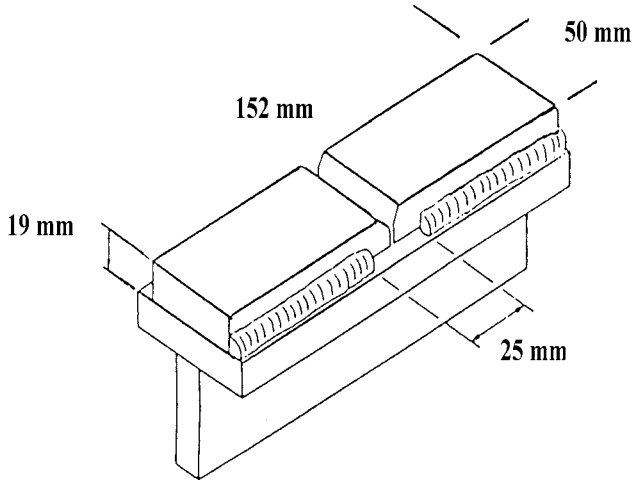


**Figure 2. Schematic illustration of the WIC test.**

**Multiple Pass Weldability Tests**

A slotted cruciform test was developed to evaluate weld metal hydrogen cracking resistance in multipass welds. Initial studies employed both 12 mm and 25 mm thick plate. The cruciform test weld design was selected because it is a high restraint configuration that is often multipass welded when used in construction. Satoh, et al. reported restraint intensity (K) measurements for a tee and cruciform type joints made with different thickness plates, reference [21]. Satoh's work showed that the cruciform design results in significantly higher restraint intensity compared to a simple tee weld using the same thickness plate.

The average stress expected in cruciform and tee weld can be calculated by multiplication of the restraint intensity by a proportionality constant m, reference [21]. The effect of plate thickness on the resulting average stress is shown in Figure 3.

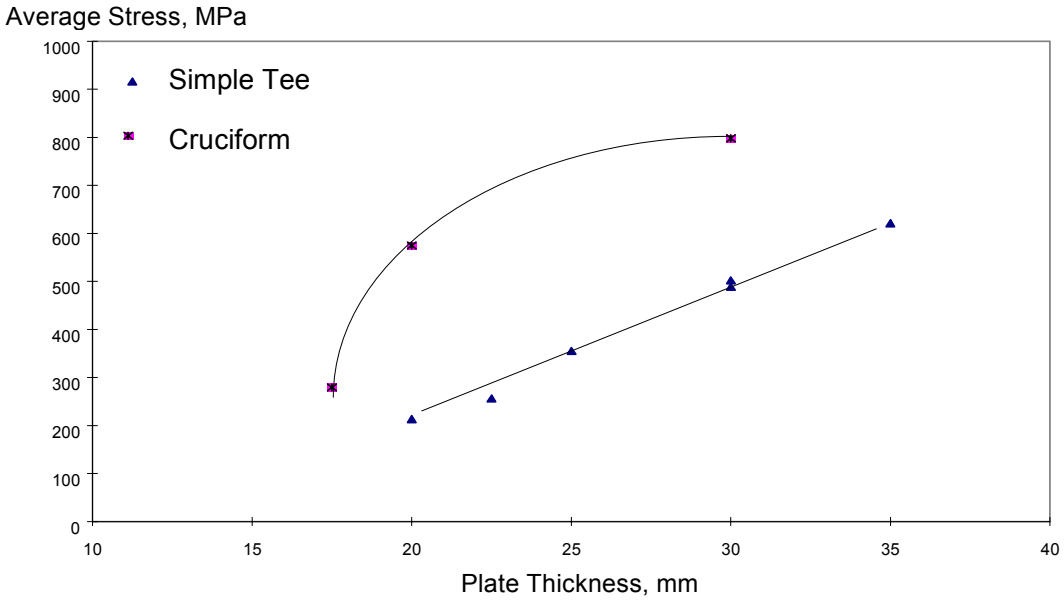


**Figure 3. Calculated average restraint stresses for a cruciform and tee weld, reference [21].**

A schematic illustration of the slotted cruciform test weld assembly (cruciform weld) used in this investigation is shown in Figure 4. As illustrated in this figure, the cruciform weld consisted of two (2) plates attached by welding to a continuous plate. One of the attached plates was un-notched. The other attached plate contained transverse and longitudinal notches shown in Figure 5. The purpose of the

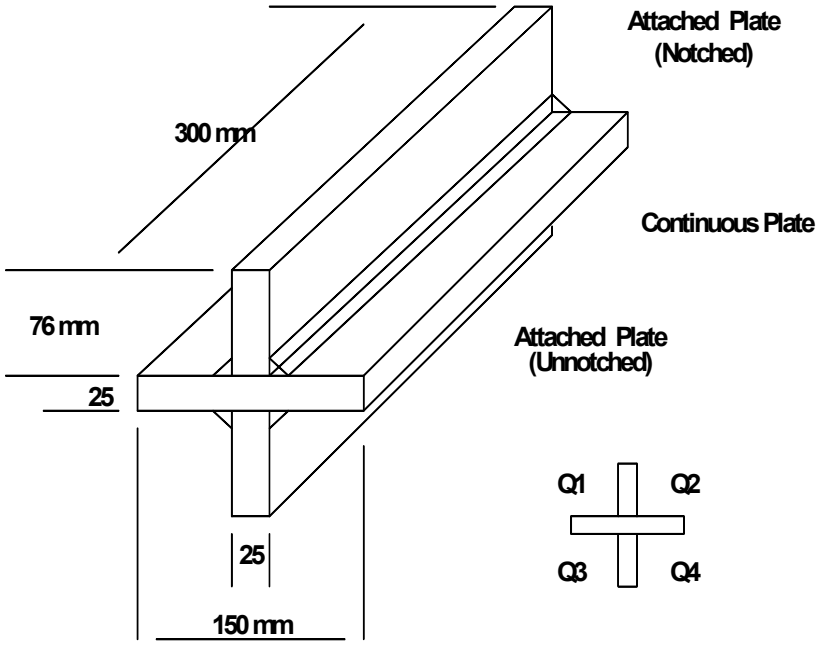


**Figure 4. Schematic illustration of the slotted cruciform test weld assembly.**

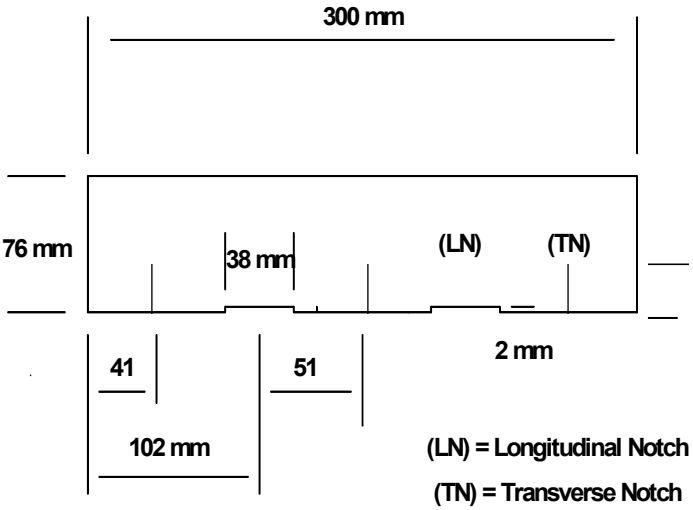


**Figure 5. Longitudinal and transverse notches in the slotted cruciform test weld assembly.**

notches was to act as hydrogen crack initiation sites. Both longitudinal and transverse notches were incorporated in the cruciform weld to contrast the frequency and extent of cracking in both the longitudinal and transverse orientation in the same specimen.

The detailed procedure used for conducting the slotted cruciform test is presented using the AWS B4.0 (Standard Methods for the Mechanical Testing of Welds) format in Appendix A. The general fabrication procedure for the cruciform test weld assembly consisted of the following steps.

1. Establish the desired preheat temperature.
2. Deposit weld beads in quadrants Q1 and Q2 (both sides of the notched attached plate, see Figure 4).
3. Re-establish the desired preheat/interpass temperature.
4. Deposit weld beads in quadrants Q3 and Q4 (both sides of the unnotched attached plate).
5. Continue steps 1 through 4 until a fillet size equal to 3/4 of the plate thickness is achieved.
6. After completion of welding, hold specimen for a minimum of 7 days (14 days were a typical hold time) prior to final magnetic particle inspection.

**Hardness, Metallography and Tensile Tests**

Rockwell C (Rc) hardness tests in the base metal, HAZ and weld metal were performed on cross sections from cruciform welds. Metallographic examinations were performed on specimens removed from HY-100, HSLA-100 and HSLA-65 cruciform welds. Examinations focused identifying and characterizing the microstructure in both the coarse grain HAZ and in the weld metal. Polished specimens were etched using a 2 percent Nital solution.

All weld metal tensile specimens (9 mm diameter) were removed from the joints in the cruciform welds attaching the un-notched plate to the continuous plate, and were tested in the as-welded condition. Tensile specimens were removed from both HY-100 and HSLA-100 cruciform welds prepared using MIL-100S and MIL-120S electrodes. After tensile testing, specimens were inspected for indications of

hydrogen embrittlement, such as reduction in ductility values (elongation and reduction of area) and signs of hydrogen damage such as fisheyes on the fracture surface or cracks on the barrel of the tensile specimen.

## RESULTS

### Thermal Severity Measurements

Thermal history is one of the factors that affects weld metal hydrogen cracking. Preheating allows the weld to cool more slowly and allows more time for hydrogen to diffuse out of the weld. A parameter used to measure this aspect of hydrogen escape is "cooling time to 100 °C" ($t_{100}$), reference [18].. In addition to increasing $t_{100}$, preheating the weld lowers the cooling rate at 573 °C, which can affect the final weld metal microstructure and hardness.

A summary of the thermal history determinations made on both cruciform and WIC test welds is presented in Table 3. As indicated in the table, for the cruciform test weld increasing the preheat temperature from 21 °C to 52 °C decreased the cooling rate at 573 °C and increased $t_{100}$. Similar trends in cooling rate at 573 °C and $t_{100}$ values were noted when preheat was increased for the WIC test welds.

Table 3. Summary of thermal history of the WIC and cruciform test welds.[1]

| Specimen | Thickness, mm | Preheat Temp. °C | Cooling Rate @ 573 °C, °C/s | Cooling time to 100 °C, sec |
|---|---|---|---|---|
| Cruciform | 25 | 21 | 52 | 120 |
| WIC | 19 | 21 | 26 | 180 |
| Cruciform | 25 | 52 | 42 | 300 |
| WIC | 25 | 52 | 23 | 300 |

1. GMAW process and 1.6 kJ/mm heat input.

As expected, considering that the same welding process and heat input were used, the larger heat sink provided by the more massive cruciform welds resulted in higher cooling rates at 573 °C compared to the WIC test welds for each preheat temperature. However, when comparing $t_{100}$ values for cruciform and WIC test welds, it is noted that when welding was accomplished using a preheat of 21 °C, cruciform welds displayed lower $t_{100}$ values or cooled faster than WIC welds. In contrast, when welding was accomplished using a 52 °C preheat temperature both the cruciform and the WIC test welds displayed the same $t_{100}$ values. The latter behavior is also attributed to the more massive cruciform welds, which retain the preheat and result in a longer time to cool to 100 °C, even though the cooling rate at 593 °C is much higher than for the WIC tests.

**Hardness Measurements**

Results of Rc hardness measurements on the base plate, HAZ and weld metal regions of samples from the cruciform welds evaluated in this study are presented in Table 4. Also shown on this table are the Pcm and CEN values calculated for the different weld metals and for the base metal and HAZ regions of these cruciform welds. As expected, the results in Table 4 indicate that Rc hardness in each region generally decreases as the Pcm and CEN value decreases.

Table 4. Rockwell C hardness measurement from slotted cruciform test welds

| Test weld | Pcm | CEN | Rc Weld | Rc plate | Rc HAZ |
|---|---|---|---|---|---|
| HY100/120S | 0.31 | 0.58 | 33.7 | --- | --- |
| HY100/100S | 0.31 | 0.53 | 28.4 | --- | --- |
| HSLA100/100S | 0.22 | 0.30 | 29.7 | --- | --- |
| HSLA100/70S | 0.22 | 0.28 | 20.7 | --- | --- |
| HSLA65/70S | 0.19 | 0.28 | 13.7 | --- | --- |
| HSLA100 | 0.31 | 0.41 | --- | 26.8 | |
| HSLA100 HAZ | 0.31 | 0.41 | --- | | 34.8 |
| HY100 | 0.30 | 0.60 | --- | 25.0 | --- |
| HY100 HAZ | 0.30 | 0.60 | --- | --- | 38.0 |
| HSLA80/100S | 0.26 | 0.36 | --- | 18.3 | --- |
| HSLA80 HAZ | 0.26 | 0.36 | --- | --- | 20.7 |
| HSLA 65 | 0.19 | 0.28 | --- | 11.3 | --- |
| HSLA65 HAZ | 0.19 | 0.28 | --- | --- | 16.6 |

To determine which chemical composition parameter, Pcm or CEN, provided a better correlation with weld metal hardness, a linear regression analysis was performed correlating Pcm and CEN to Rc hardness. Results of these analyses are presented in Figures 6 and 7, which also indicate the Pearson coefficient of determination ($R^2$) values for the base plate, HAZ and weld metal. As indicated by the results presented in these figures and summarized in Table 5, the correlation between base plate, HAZ and weld metal Rc hardness and Pcm is consistently stronger than that between Rc hardness for the same regions and CEN. Although the correlation coefficient for both CEN and Pcm to weld metal hardness was low (0.52 and 0.60 respectively), based on the stronger overall correlations with hardness, Pcm was selected as the hardenability indicator for the weld metal cracking prediction model developed

in this investigation. It is noted that the large variation in weld metal to hardness noted above is typical for weld metals due to grain boundary orientation effects and multiple thermal cycles.

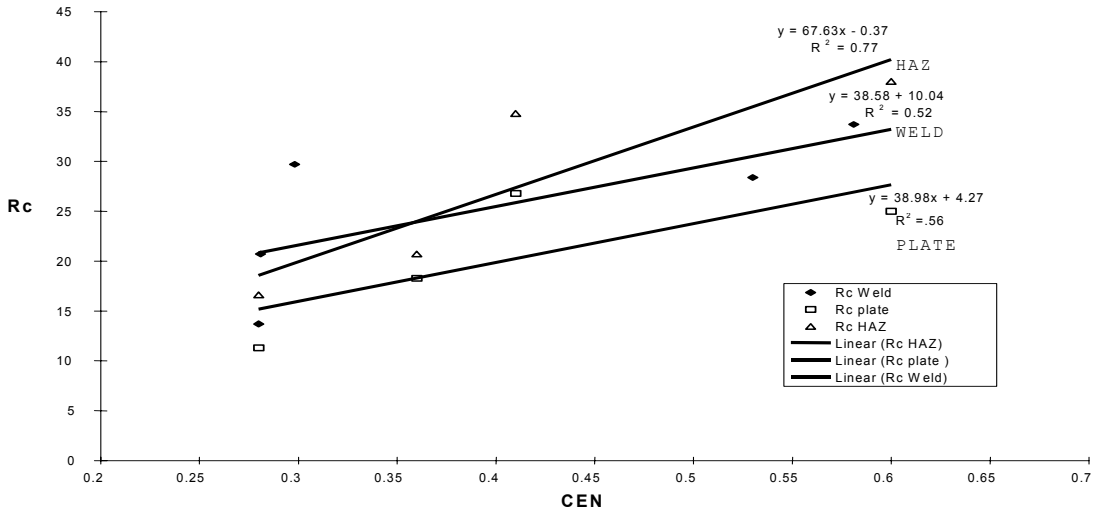


**Figure 6. Correlation of Pcm values to Rockwell C hardness.**

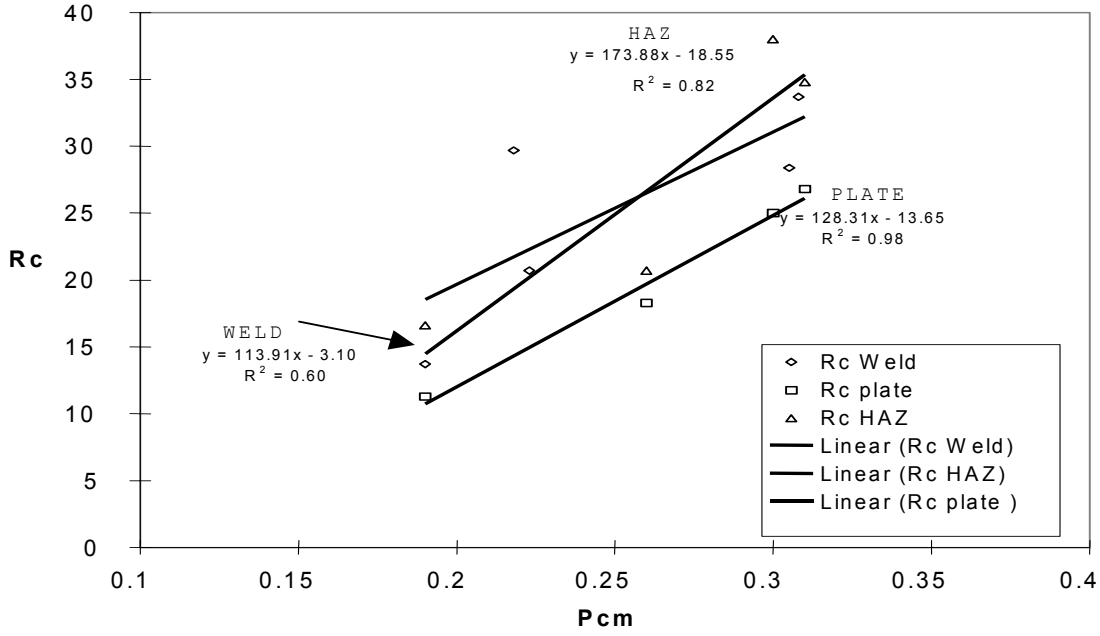


**Figure 7. Correlation of CEN values to Rockwell C hardness.**

Table 5. Summary of correlations between Pcm and CEN and Rc hardness

| Material | $R^2$ | |
|---|---|---|
| | Pcm | CEN |
| Base Plate | 0.98 | 0.56 |
| HAZ | 0.82 | 0.77 |
| Weld Metal | 0.60 | 0.52 |

**Metallography**

Metallographic specimens were removed from selected cruciform test welds and etched with a 2 percent Nital solution. Photomicrographs of the coarse grain HAZ of HY-100, HSLA-100 and HSLA-65 are shown in figures 8, 9 and 10, respectively. The HY-100 HAZ microstructure has been reported to be primarily tempered martensite, reference [22]. The HAZ of the HSLA-100 appeared to exhibit a finer grain size compared to the HY-100. Some investigators have described the microstructure of the HSLA-100 HAZ as low carbon upper bainite and martensite, reference [23]. The HAZ from the HSLA-65 appeared slightly coarser than the HAZ of the other steels.

Photomicrographs of the MIL-120S, MIL-100S, and MIL-70S weld metal are shown in figures 11, 12 and 13, respectively. The MIL-120S product was developed to produce an upper bainite microstructure in the fusion zone, reference [24]. MIL-100S was also designed to produce a banitic microstructure, except that the material transforms at a higher temperature resulting in a coarser microstructure than MIL-120S, reference [24]. The MIL-70S weld metal exhibited a coarser microstructure compared to the other two weld metals. Despite the slightly coarser microstructure , there were still fine acicular features observed in the MIL-70S microstructure.

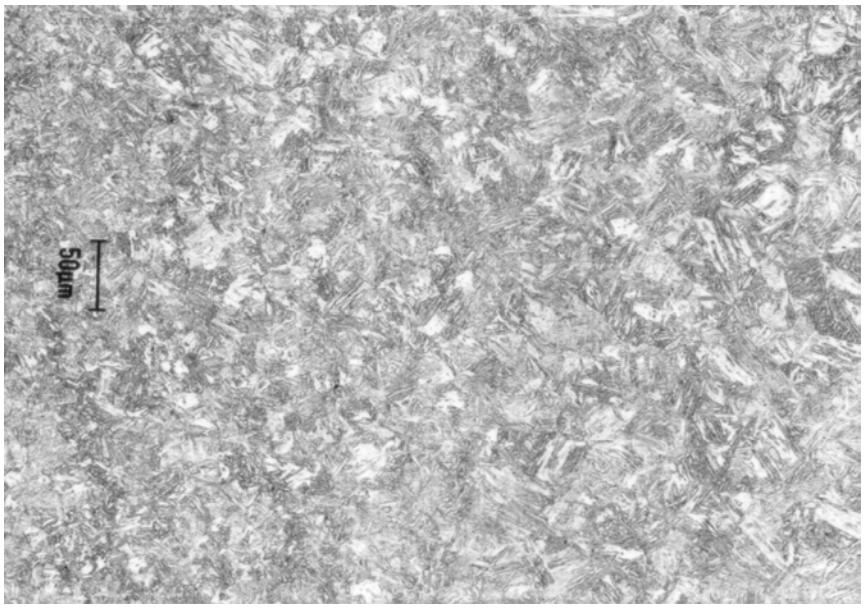


**Figure 8. Photomicrograph of the coarse grained HAZ in HY-100 (W345).**

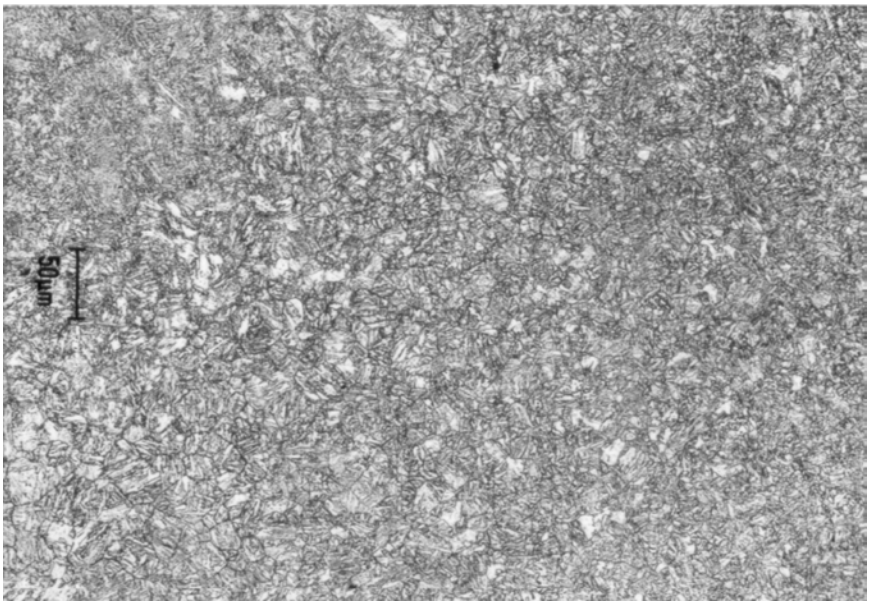


**Figure 9. Photomicrograph of the coarse grained HAZ in HSLA-100 (W341).**

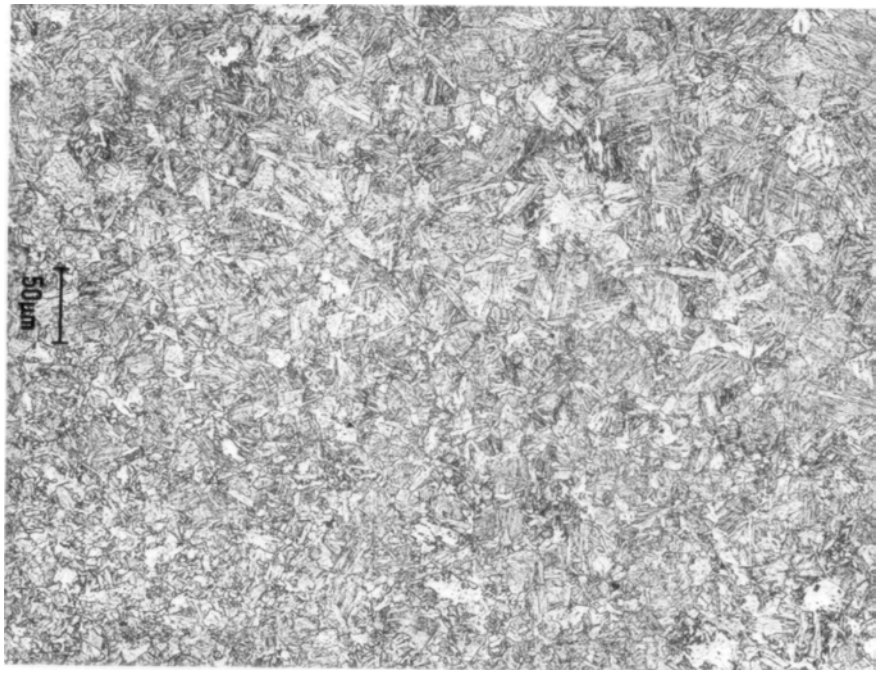


**Figure10. Photomicrograph of coarse grained HAZ in HSLA-65 (W353).**

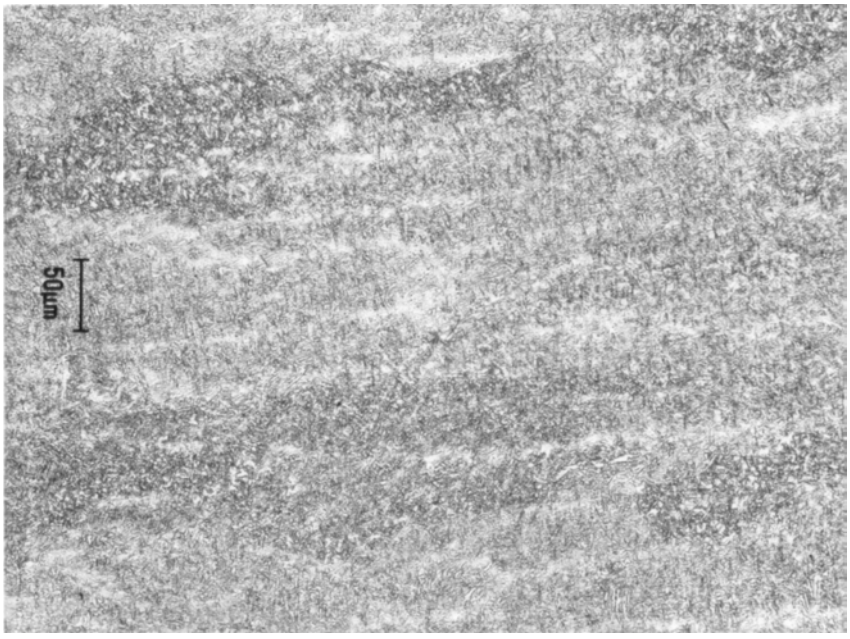


**Figure 11. Photomicrograph of MIL-120S weld metal (W345).**

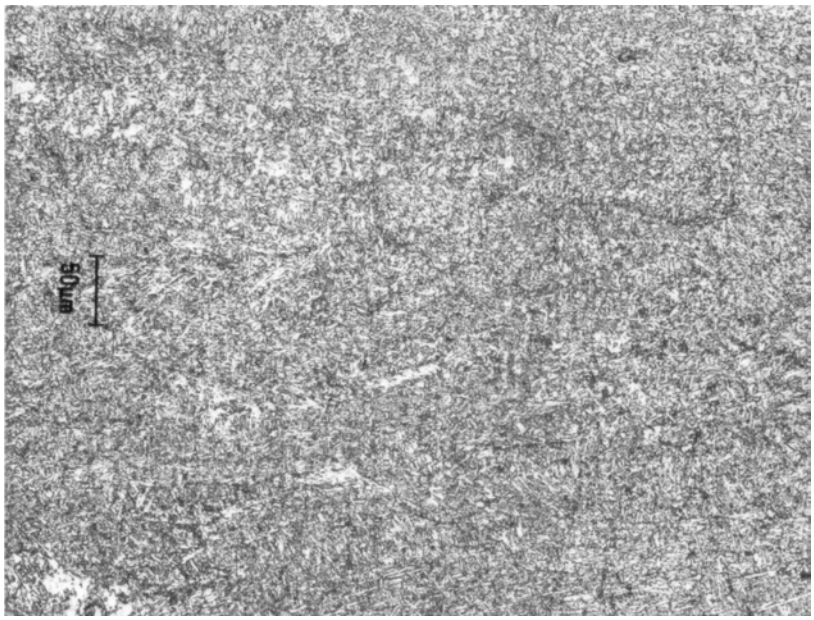


**Figure12. Photomicrograph of MIL-100S weld metal (W341).**

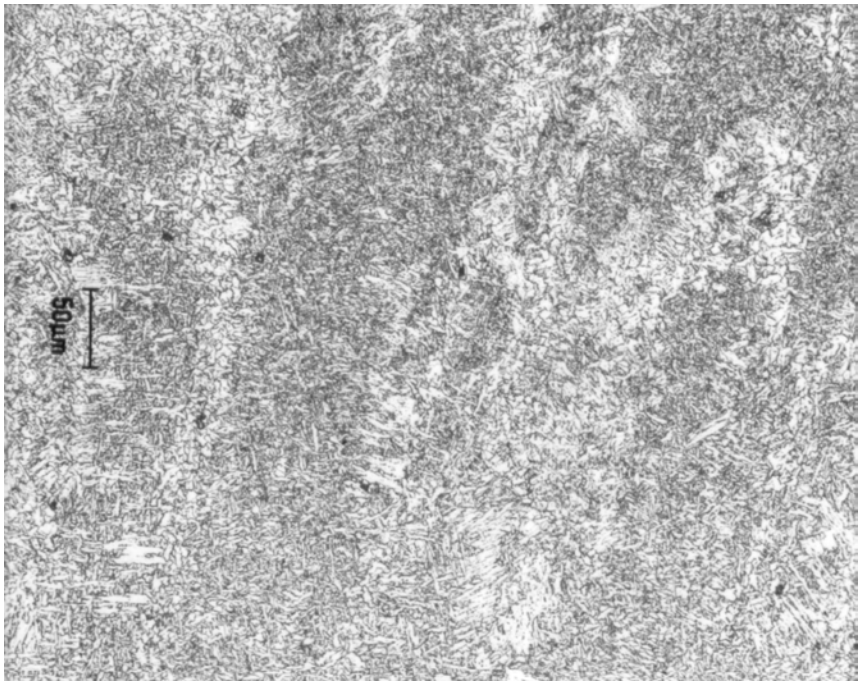


**Figure 13. Photomicrograph of MIL-70Sweld metal (W353).**

**WIC Test Results**

A series of WIC tests were performed using the materials identified in Tables 1 and 2. All tests were conducted using a welding heat input of 1.6kJ/mm, but different preheat temperatures were used to obtain a range of $t_{100}$ values. The relationship between $t_{100}$ and Pcm carbon equivalent on weld metal cracking resistance is shown in Figure 14. In these tests the diffusible hydrogen contents were all approximately 5 to 6 ml/100g as measured by a gas chromatography technique following the procedures in reference [26]. The line in Figure 14 delineates the cracking and no cracking regions, and indicates that as Pcm increases, the $t_{100}$ value needs to be increased in order to avoid cracking. Consequently, the line in Figure 14 is defined as $t_{100,\ critical}$ and indicates the minimum $t_{100}$ value required to avoid cracking for a given weld metal composition. The line in Figure 14 is defined by equation (3) below.

Equation (3) $t_{100,\ crit} = (111)\ Pcm - 23.3$

Where Pcm is given in Equation (1)

Another series of WIC specimens was evaluated using the GMAW process, a welding heat input of 1.6kJ/mm and a 21ºC preheat temperature. For this series of tests, the diffusible hydrogen content was varied. The variation in Hd values was accomplished by using M-2 shielding gas with 0.0, 0.3, 0.6, or 0.9 percent hydrogen gas premixed in the bottle by the shielding gas distributor. The slope of the line in Figure 15 represents the relative change in Hd as a function of changes in Pcm ($\Delta Hd / \Delta Pcm$). The numerical value of the slope is approximately -110. The reciprocal negative slope of the line in Figure 15 can be interpreted to indicate that an increase in Pcm requires a decrease in Hd in order to maintain similar hydrogen cracking resistance.

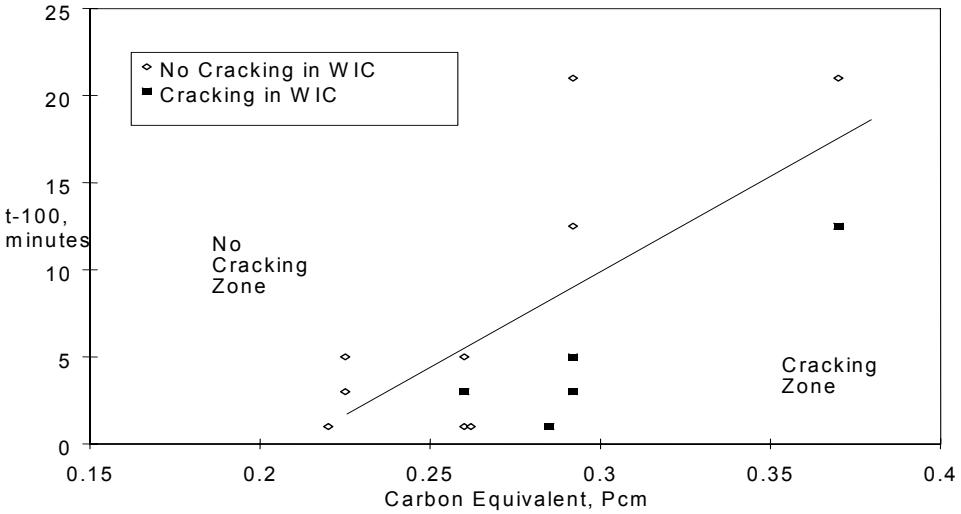


**Figure 14. Effect of $t_{100}$ and Pcm on weld metal hydrogen cracking in the WIC test welds.**

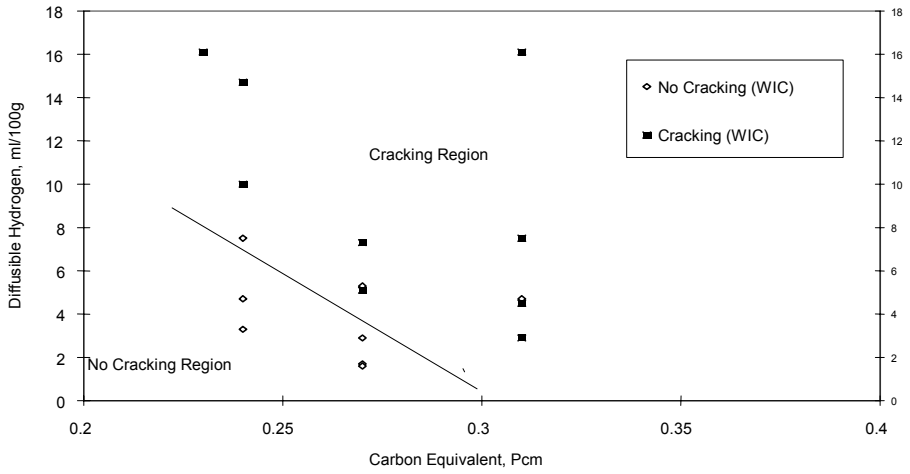


**Figure 15. Effect of Hd and Pcm on weld metal hydrogen cracking in the WIC test welds.**

Multiplying the reciprocal negative slope coefficient of 1/110 by the Pcm coefficient ( = $\Delta t_{100}$ / $\Delta$ Pcm) in Figure 14 (i.e. 111) determines the effect (coefficient) of independent Hd variable on the $t_{100, crit}$. dependent variable. This relationship is expressed by Equation (4).

Equation (4) $$\frac{\Delta t_{100}}{\Delta Hd} = \frac{\Delta Pcm}{\Delta Hd} * \frac{\Delta t_{100}}{\Delta Pcm} = \frac{(110)}{(111)} = 0.99$$

Combining equations (3) and (4) and assuming the linear relationships among $t_{100}$, Pcm and Hd results in a response surface describing the minimum or critical "cooling time to 100 C" necessary to avoid hydrogen cracking ($t_{100,crit}$) due to changes in both Pcm and diffusible hydrogen content (Hd). The relationship between Pcm, Hd, and $t_{100,crit}$ is given by Equation (5) and is illustrated in Figure 16.

Equation (5) $$t_{100, critical} = (111)\ Pcm + (0.99)\ Hd - 28.25$$

where Pcm is given in Equation (1)

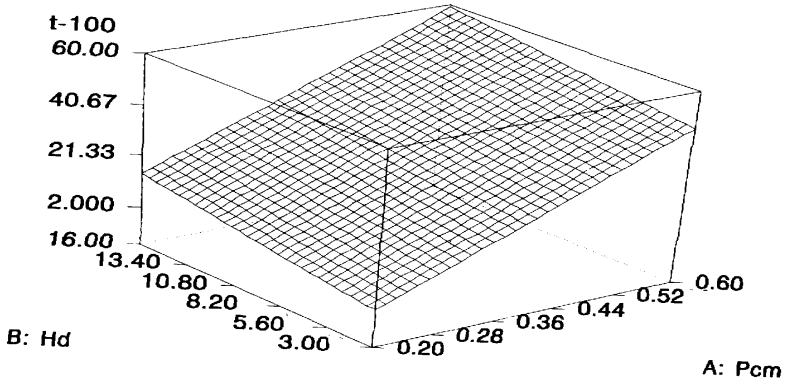


**Figure 16. Minimum critical cooling time to avoid weld metal hydrogen cracking as a function of Hd and Pcm.**

**Slotted Cruciform Test Results - Tensile Tests**

All weld metal (AWM) 9 mm round tensile specimens were removed from quadrants 3 and 4 of the cruciform welds (the un-notched side of the specimen shown in Figure 4). Initial tensile tests were performed on specimens from HSLA-100 and HY-100 cruciforms welded using a 21ºC preheat and interpass temperature and MIL-120S and MIL-100S electrodes.. Results shown in Table 6 indicate that the high cooling rate resulting from welding a 25 mm thick cruciform using a 21ºC preheat and interpass temperature resulted in very high weld metal yield strength values in both MIL-120S and MIL-100S weld metal.

Hydrogen damage was found in the MIL-120S all weld metal tensile specimens. The hydrogen damage resulted in low elongation and reduction of area values in specimens from weld W345 (Table 6). Hydrogen flakes were observed on fracture surfaces and checkered cracking was seen on the barrel of the tensile specimens from weld W345. An example of the cracking observed on the barrel of the tensile specimens is shown in Figure 17. Although MIL-120S weld metal tensile ductility values from weld W352 were relatively high, there was evidence of hydrogen damage on the tensile fracture surfaces.

Table 6. All weld metal tensile test results from slotted cruciform welds.

| ID | Plate | Electrode | 0.2% Y.S. MPa | U.T.S. MPa | El. % | R.A. % | Fracture |
|---|---|---|---|---|---|---|---|
| W345 | HY-100 | MIL-120S | 868 | 951 | 6* | 18 | Shear* |
| W352 | HSLA-100 | MIL-120S | 950 | 1070 | 23 | 61 | cup/cone* |
| W343 | HY-100 | MIL-100S | 814 | 879 | 20 | 69 | cup/cone |
| W341 | HSLA-100 | MIL-100S | 806 | 910 | 21 | 69 | cup/cone |
| | | | | | | | |

*Hydrogen damage was observed in the specimen

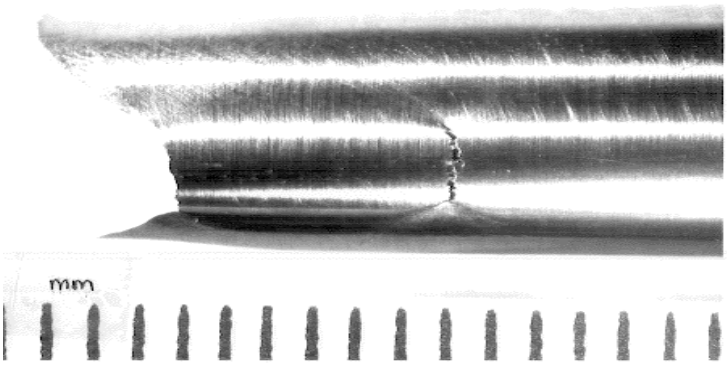


**Figure 17. Hydrogen cracking observed on the barrel of an MIL-120S all weld metal tensile specimen.**

To confirm that the damage to the MIL-120S weld metals was caused by hydrogen, additional tensile specimens were tested after being subjected to a hydrogen removal heat treatment. An additional set of tensile specimens was removed from cruciform weld W352. Since no remaining material was available from cruciform weld W345, an additional cruciform weld (W351) was fabricated using the same materials welding parameters used for weld W351. Coupons from these welds were subjected to a post weld hydrogen removal heat treatment that consisted of baking the coupons at 177 °C for 24 hours. Tensile test results are summarized in Table 7 and indicate that there was no evidence of hydrogen damage on any of the heat treated tensile specimens.

Table 7. Tensile test results of MIL-120S weld metal after a post weld heat treatment

| ID | Plate | Electrode | 0.2% Y.S. MPa | U.T.S. MPa | El. % | R.A. % | Fracture |
|---|---|---|---|---|---|---|---|
| W351HT | HY-100 | MIL-120S | 888 | 923 | 25 | 65 | cup/cone |
| W352HT | HSLA-100 | MIL-120S | 885 | 924 | 24 | 65 | cup/cone |

**Weld Cracking**

Initial cruciform test welds employed a MIL-100S electrode and HSLA-100 or HY-100 plate materials and included the use of two types of cruciform welds. The first type of test weld was a standard cruciform using 12 mm thick plates, without any notches. The second type of cruciform used 25 mm thick plates and contained machined notches as shown in Figure 5 All the initial cruciform welds were prepared using the GMAW process, a 1.6kJ/mm heat input and a 21ºC preheat and interpass temperature.

Examination of the 12 mm cruciform welds did not reveal any indications of cracking. Cracking observed in the 25 mm cruciform is discussed in more detail below. Since no cracking was observed in the 12 mm cruciform tests, no other 12 mm cruciform tests were conducted.

One of the purposes of the slotted cruciform design was to compare longitudinal and transverse weld metal cracking resistance in a multiple pass weld. Cross section examination for longitudinal and transverse cracking was accomplished by sectioning perpendicular to the plane of the notch, through the center of the notch. A schematic illustration of how the longitudinal and transverse notched specimens were sectioned is shown in Figure 18.

The longitudinal notched specimens produced cracks parallel to the direction of welding. A macrosection of the longitudinal notch and a longitudinal heat affected zone crack is shown in Figure 19. Examination of the transverse notch involved first sectioning the specimen approximately 2-3 mm in front of and behind the transverse notch. The specimen is then sectioned perpendicular to the plane of the transverse notch approximately halfway up the vertical leg of the fillet weld as illustrated in Figure 20, which also shows a transverse weld metal crack emanating from the notch.

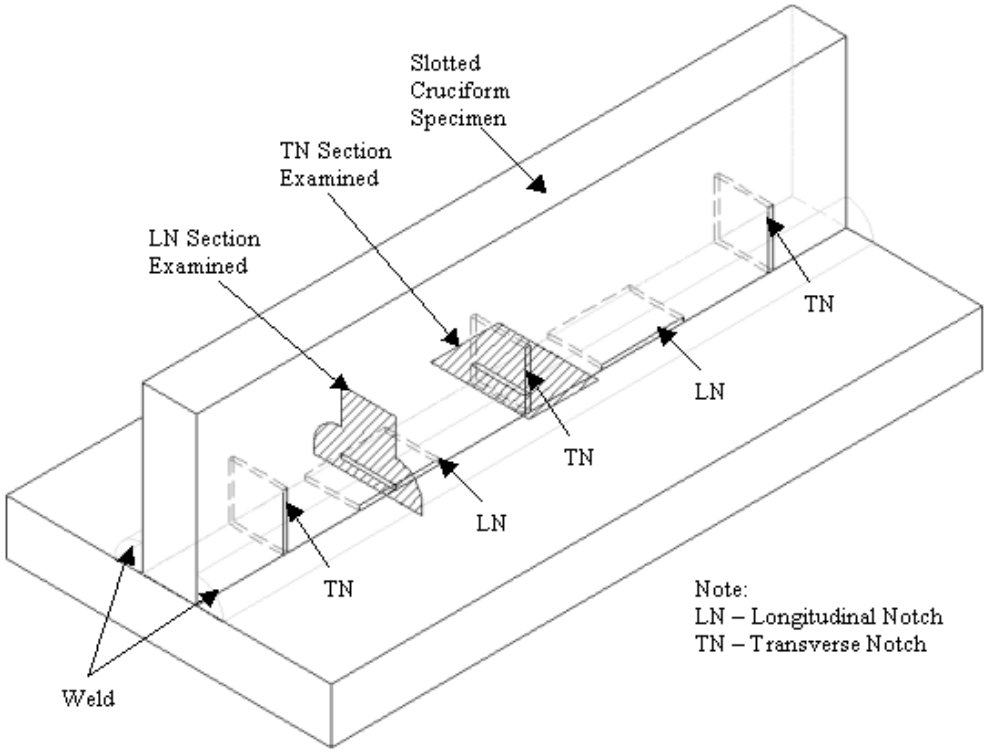


**Figure 18. Schematic illustrating how the longitudinal and transverse notched specimen were sectioned.**

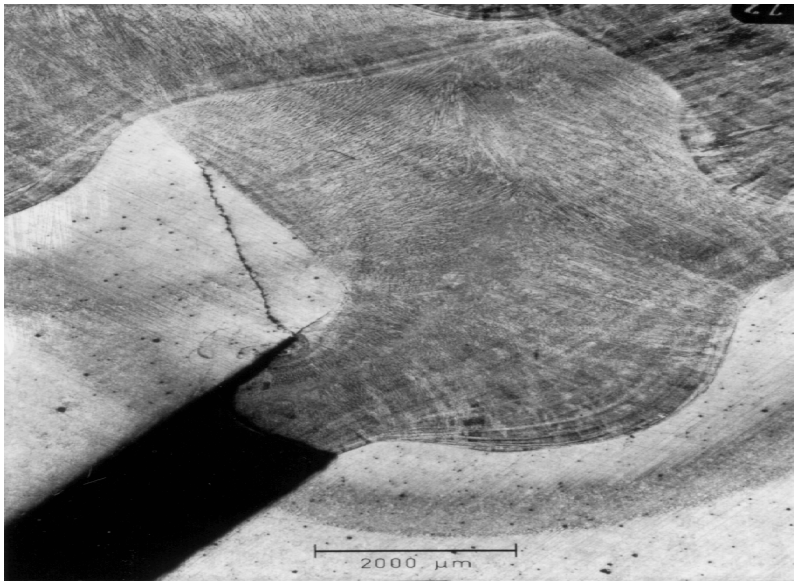

**Figure 19. Example of HAZ zone cracking observed from a longitudinal notch in cruciform weld W342.**

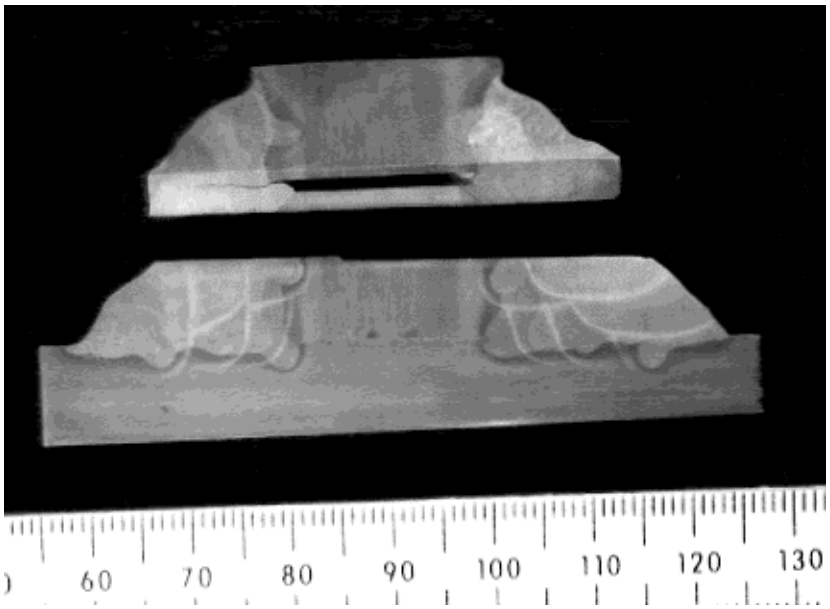


**Figure 20. Example of weld metal cracking observed from a transverse notch in cruciform weld W351.**

In some MIL-120S cruciform welds prepared using a 21ºC preheat and interpass temperature weld metal hydrogen cracking was observed away from the notches. An example of these weld metal cracks is shown in Figure 21. The fracture surface of a weld metal hydrogen crack is shown in Figure 22. In addition to the intergranular and branched cracking shown in Figure 22, there were also regions that appeared roughly striated on a macroscopic level. These areas may have fractured along the original solidification cell boundaries.

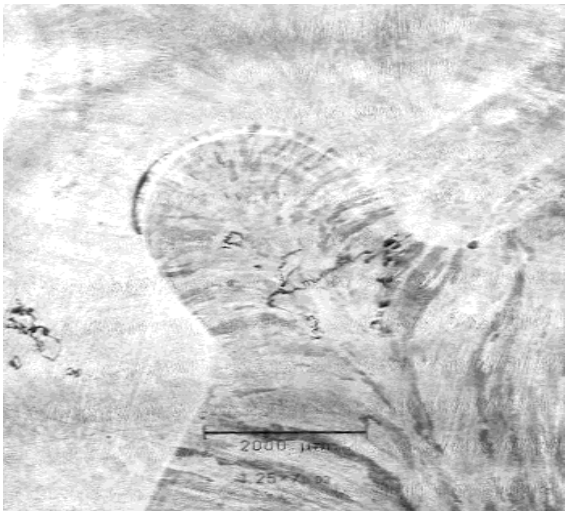

**Figure 21. Weld metal cracking in weld W352 fabricated with a MIL-120S electrode.**

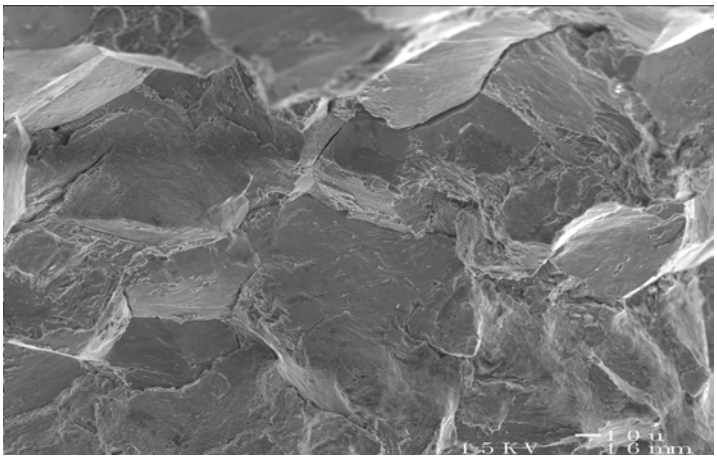


**Figure 22. Fractograph of a MIL-120S weld metal hydrogen crack from cruciform weld W351.**

A summary of the cruciform welds fabricated using a 21ºC preheat and interpass temperature is provided in Table 8. No weld metal cracking was observed in the welds prepared using MIL-100S electrodes. In some instances small HAZ cracks (0.5 to 3 mm long) were noted at longitudinal notches in the HY-100 and HSLA-100 specimens next to the MIL-100S weld deposit. As indicated in Table 8, cruciform specimens fabricated with the MIL-120S electrode exhibited both weld metal and HAZ cracks at longitudinal notches and weld metal cracks at transverse notches. MIL-120S weld metal cracks initiating at transverse notches were significantly larger than the cracks at longitudinal notches. The observation of small HAZ cracks in the HSLA-100 slotted cruciform specimens is somewhat surprising

in view of prior Navy research, reference [10], and the extensive successful experience in welding this material in Navy ship construction. These cracks are attributed to the combined effects of thermal severity (i.e., cooling rate at 573ºC of 52ºC/sec and relatively low $t_{100}$) of the welding conditions and the presence of the mechanical notch.

The HSLA-80 plate / MIL-100S electrode and HSLA-65 plate / MIL-70S electrode cruciform welds prepared using a 21ºC preheat and interpass temperature did not exhibit any cracking. This improved hydrogen cracking resistance is attributed to the significantly lower HAZ and weld metal (for MIL-70S) hardness and to the lower Pcm values (HSLA-80, HSLA-65 and MIL-70S) compared to the HY-100 and HSLA-100 cruciform welds. It should be noted that specimen W355 was fabricated to determine the effect of higher hydrogen levels on hydrogen cracking resistance of the HSLA-80 /MIL-100S system. This specimen was welded with an argon-2 percent oxygen shielding gas that had 0.3 percent hydrogen premixed in the gas bottle prior to welding. This doubled the diffusible hydrogen content in the weld, raising it to 12 ml/100g. The results in Table 8 show that small (1 to 2 mm) weld metal cracks were present. These results suggest that weld metal hydrogen cracking can occur in relatively weldable materials at sufficiently high hydrogen levels. No cracks were observed in the HSLA-80 HAZ.

To determine if the cracking observed in the HY-100 / HSLA-100 cruciform welds was due to the thermal severity of the welding conditions used to fabricate the welds identified in Table 8,

Table 8. Results of slotted cruciform welds fabricated using a 21°C preheat / interpass temperature.

| Weld ID | Plate | Electrode | Longitudinal Notch, Crack location/length | Transverse Notch, Crack location/length |
|---|---|---|---|---|
| W341 | HSLA-100 | MIL-100S | HAZ/2mm | None |
| W342 | HSLA-100 | MIL-100S | HAZ/3mm | None |
| W343 | HY-100 | MIL-100S | HAZ/0.5mm | None |

| | | | | |
|---|---|---|---|---|
| W344 | HY-100 | MIL-100S | HAZ/1mm | None |
| W345 | HY-100 | MIL-120S | Weld/1mm and 5mm, HAZ/1mm | Weld/8mm |
| W351 | HY-100 | MIL-120S | Weld/2mm and 4mm | Weld/13mm |
| W352 | HSLA-100 | MIL-120S | Weld/3mm and 6mm, HAZ/2mm | Weld/8mm and 13mm |
| W356 | HSLA-80 | MIL-100S | None | None |
| W355* | HSLA-80 | MIL-100S | Weld/1mm* | Weld/2mm* |
| W353 | HSLA-65 | MIL-70S | None | None |

* Specimen W355 was fabricated with 0.3% hydrogen in the shielding gas that resulted in an Hd of 12 ml/100g. This is twice the normal Hd level.

additional slotted HY-100 and HSLA-100 cruciform welds were fabricated using a higher preheat and interpass temperature (52 °C). As indicated from the results of these tests, summarized in Table 9, there was no cracking in any of these welds. Thus, increasing the preheat and interpass temperature appears to have reduced the thermal severity of welding conditions sufficiently to prevent hydrogen cracking in these welds.

Table 9. Results of slotted cruciform welds fabricated using a 52ºC preheat / interpass temperature.

| Weld ID | Plate | Electrode | Longitudinal Notch Crack location/length | Transverse Notch Crack location/length |
|---|---|---|---|---|
| W346 | HSLA-100 | MIL-100S | None | None |
| W347 | HSLA-100 | MIL-100S | None | None |
| W348 | HY-100 | MIL-100S | None | None |
| W349 | HY-100 | MIL-100S | None | None |
| W350 | HY-100 | MIL-120S | None | None |

Results of the cruciform tests were superimposed on the results of the WIC tests as shown in Figure 23. Results of cracking and no cracking conditions in the cruciform test fall into a similar cracking and no cracking zone initially established by the WIC results and indicate that the crack prediction equation given by Equation (5) is a suitable approximation for cracking versus no cracking in a multipass welding situation such as the slotted cruciform test. The response surface shown in Figure 16 is useful to observe the relative effects of Pcm and Hd on $t_{100,crit}$. It is also useful to analyze the results in a plan view. An example of a plan view of Equation (5) is given in Figure 24. An example of using Figure 24 is as follows: projecting a vertical line from Pcm = 0.26 and a horizontal line at Hd = 9.5 indicate that with these conditions a minimum $t_{100}$ of approximately 15 minutes is recommended to avoid cracking. Nomographs or other guidelines can then be used to determine plate thickness and welding conditions necessary to meet this minimum cooling time, reference [18].

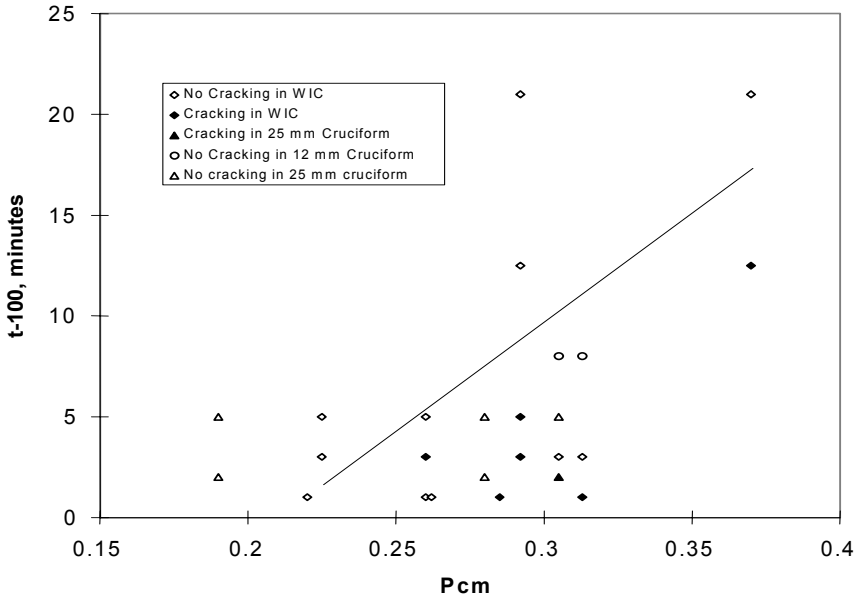


**Figure 23. Effect of $t_{100}$ and Pcm on cracking in WIC and cruciform tests.**

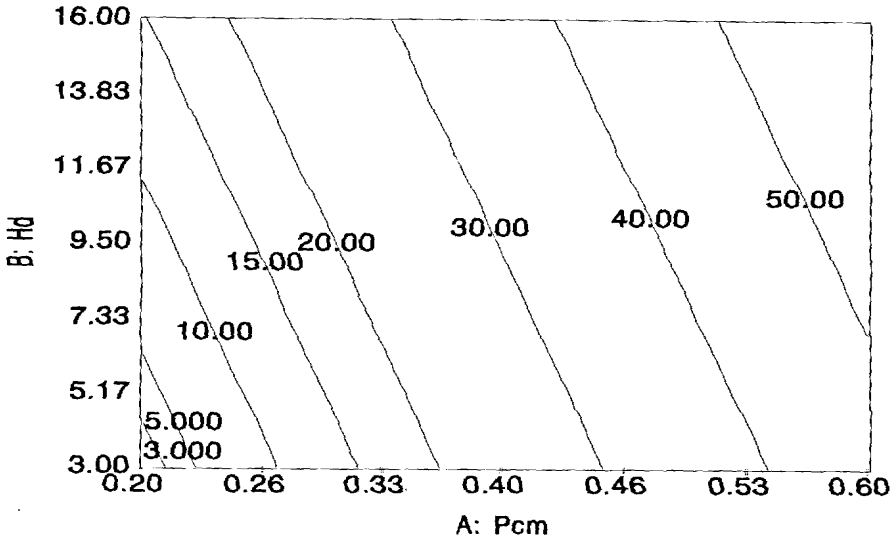


**Figure 24. Projection of iso-$t_{100}$ lines.**

## Summary and Conclusions

1. The single pass WIC weldability test was used to establish weld metal cracking versus no cracking conditions as a function of changes in chemistry and diffusible hydrogen content. The critical level of hydrogen that results in weld metal cracking was found to decrease as the calculated Pcm value increased (Figure 15).
2. Results from single pass and multiple pass weldability tests were used to develop a weld metal hydrogen crack prediction model (Equation (5)). The model identifies the critical cooling time ($t_{100crit.}$) required to avoid weld metal hydrogen cracking, when the weld metal chemical composition and diffusible hydrogen level are known.
3. The weld metal cooling rate at 573ºC in the multiple pass cruciform specimen design was found to be greater than in single pass WIC type weldability tests.
4. Results from slotted multipass cruciform test welds indicated transverse weld metal hydrogen cracks were significantly larger than longitudinal cracks when both types of cracking occurred. Tensile testing of all weld metal samples removed from the cruciform specimen was useful for showing hydrogen embrittlement by the loss of tensile ductility.
5. MIL-120S weld metal exhibited hydrogen cracking and hydrogen damage on all weld metal tensile specimens when welded without preheat. Increasing the preheat and interpass temperature to 52 °C eliminated this problem.

# APPENDIX A

# SLOTTED CRUCIFORM TEST PROCEDURE

## 1. Scope

**1.1** The cruciform test is used to measure the susceptibility to hydrogen cracking of steel weldments, primarily focusing on fillet weld applications. While the primary application is to evaluate base-metal composition, the test also may be used to evaluate the effects of welding consumables, welding heat input, preheating, and post-heating , on cracking susceptibility.

**1.2** This standard is applicable to the following:

(1) Qualification of materials and welding procedures where specific acceptance standards have been specified.
(2) Information, basis of acceptance or manufacturing and quality control
(3) Research and development

**1.3** The use of this test is restricted as follows:

(1) The test shall not be used for base metal less than 12mm (1/2 in.) thick.

(2) Close control of all welding conditions is required. The results of this test may be strongly affected more by changes in welding conditions.

**1.4** The following information shall be furnished:

(1) Test number

(2) Welding procedure specification and procedure qualification record if applicable

(3) Base metal specification/identification, thickness, and actual chemical composition

(4) Filler metal specification/identification, size and any pre-welding treatment, e.g. baking time and temperature.

(5) Type and flow rate of any shielding gas used.

(6) All welding procedures (process and parameters).

(7) Any preheat / interpass temperature and post-heating treatment used.

(8) Acceptance criteria.

(9) The number of cross sections to be examined.

**1.5 Safety Precautions.** Safety precautions shall conform to the latest edition of ANSI/ASC Z49, Safety in Welding, Cutting, and Allied Processes, published by the American Welding Society.

**2**. **Applicable Documents**

Reference should be made to the latest edition of the following documents:

| | |
|---|---|
| ANSI/AWS A2.4 | Standard Symbols for Welding, Brazing, and Nondestructive Examination |
| ANSI/AWS A3.0 | Standard Welding Terms and Definitions |
| ANSI/AWS A4.3 | Standard Methods for Determination of the Diffusible Hydrogen Content of Martensitic, Bainitic, and Ferritic Steel Weld Metal Produced by Arc Welding |

The sources for these documents are the following

American Welding Society (AWS)

550 N.W. LeJeune Road

Miami, Florida 33126

**3**.**Summary of Method**

**3.1** The test specimen consists of three plates tack welded at their ends to form a double T-joint (Figure A1).

**3.2** One of the attached plates contains longitudinal and transverse notches.

**3.3** A multiple-pass fillet weld is deposit in succession in each of the four quadrants. Each weld pass is allowed to cool to the desired interpass temperature prior to depositing the subsequent bead. After the welding is completed, the specimen is given any specified post-weld treatment.
**3.4** The completed welds are examined visually for any external cracks and the specimen is sectioned transversely for metallographic examination for hydrogen cracks.

**4. Significance**

This test is relatively severe for detecting hydrogen cracks. The welding conditions must be very closely controlled to avoid any variations that may result in inconsistent results. Multiple specimens may be required to assure reliable assessment of the cracking susceptibility.

**5**. **Definitions and Symbols**

The welding terms used in this standard are in accordance with the latest edition of ANSI/AWS A3.0, Standard Welding Terms and Definitions

**6. Apparatus**

Evaluation for the presence of hydrogen cracks requires the use of metallographic equipment to section and prepare the specimen for examination.

**7. Specimens**

The test specimen is shown in Figure A1. The recommended base plate thickness is 25 mm (1 in.). Thicker plate may also be employed (depending on the desired application). The two surfaces of Plate A are ground to bright metal prior to assembly. The mating edges of Plates B and C are machined flat prior to assembly. This is essential to insure intimate contact and good heat transfer between these surfaces during welding of the assembled specimen. Notches are machined on the edge of the plate as shown in Figure A1. The assembly is tack welded together prior to the test.

The suggested minimum dimensions of the plates for the slotted cruciform specimens are shown below:

| | Thickness, mm | Length, mm | Width, mm |
|---|---|---|---|
| Continuous Plate A | 25 | 300 | 300 |
| Attached Plate B (Slotted) | 25 | 300 | 150 |
| Attached Plate C (Unslotted) | 25 | 300 | 150 |

**8. Procedure**

**8.1** Test welds are deposited in the sequence shown in Figure A2. All welding shall be done in the flat position unless otherwise specified. A mechanized process may be used to maintain control of the welding parameters.

**8.2** All test welds are deposited in the same direction of travel. Each weld is made without any arc interruptions and the craters at the ends of the test are to be filled before the arc is extinguished. The same welding parameters are used for each test weld and each weld should be of the same size.

**8.3** The fabrication sequence is as follows: (1) Establish desired preheat temperature. (2) For the first pass (root pass) in each quadrant deposit a weld bead on each side of the attached plate. For example, weld quadrants 1 and 2, one after another. (3) Establish desired interpass temperature. (4) Weld the root pass in quadrants 3 and 4, one after another. (4) Re-establish interpass temperature. (5) Deposit a second weld bead in quadrant 1. (6) Re-establish interpass temperature. (7) Deposit a second weld bead in quadrant 2. (8) Re-establish interpass temperature prior to each weld pass (unlike the root passes that are welded in pairs). (7) Continue welding until a fillet size that results in a 100 percent efficient joint is achieved (typically ¾ t, where t is thickness of plate).

**8.4** If weld metal cracking occurs in any of the test welds, the test shall be discontinued and the location and extent of cracking noted on the test record sheet.

**8.5** If the welding procedure requires preheating, the specimen shall be preheated before depositing each test weld. If post-weld heat treatment is required, the treatment shall be applied to the test weldment immediately after completion of welding and before cooling to ambient temperature. If no post-weld

heat treatment is required, the as-welded specimen shall be aged at ambient temperature for 7 to 14 days or as specified by the customer.

**8.6** The weldment is sectioned and examined for cracks. Macrosections are cut transverse to the direction of welding from the weldment, preferably by using a water-cooled band saw or abrasive cut-off wheel. Each macrosection shall be identified as to its location in the test weldment and the four quadrants corresponding to the fabrication sequence shall be identified.

**8.7** As illustrated in figure A3, the longitudinal areas, the transverse macrosections may be examined directly in this orientation. For the transverse notched areas, each specimen is first sectioned parallel to the plane of the transverse notch approximately 3 mm in front of and behind the notch. The specimen is then sectioned perpendicular to the first cuts halfway up the vertical leg of the fillet weld. The face of the section to be examined is polished etched, and examined at 50 X or greater magnification. The location and size of any cracks shall be recorded.

**8.8** A diffusible hydrogen test shall be performed for each welding process and consumable in accordance with ANSI / AWS A4.3. The diffusible hydrogen test should be performed under the same ambient condition as the cruciform test weldment.

**9. Report**

**9.1** The test results that typically are reported are the following:

(1) Base metal and filler metal identification and chemical composition

(2) Base metal (specimen) thickness

(3)Welding procedures (process and parameters)

(4) Any preheating and/or post-weld heat treatment

(5) Weld fillet size for multipass welds

(6) Identification of each section cut from the specimen and each quadrant in the section

(7) Location and size of any cracks in each test weld in each section.

(8) Results of diffusible hydrogen test.

(9)Test data should be recorded on a Test Record Sheet similar to Figure A5

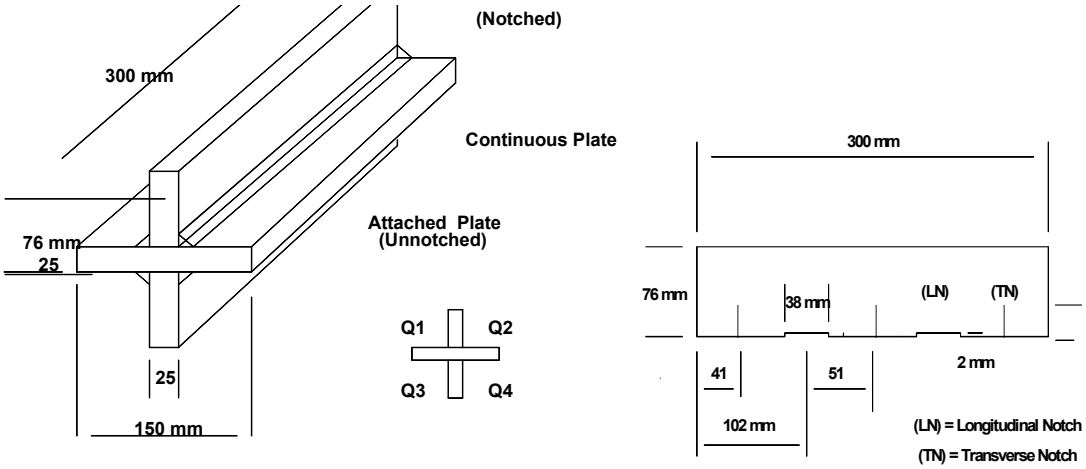


Figure A1. Schematic illustration of cruciform test assembly

Plate B

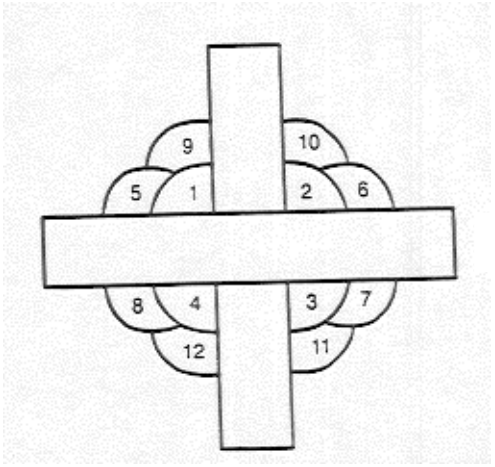


Plate A

Plate C

Figure A2. Fabrication Sequence (only first two layers shown, more may be needed for thicker plate, see section 8.3)

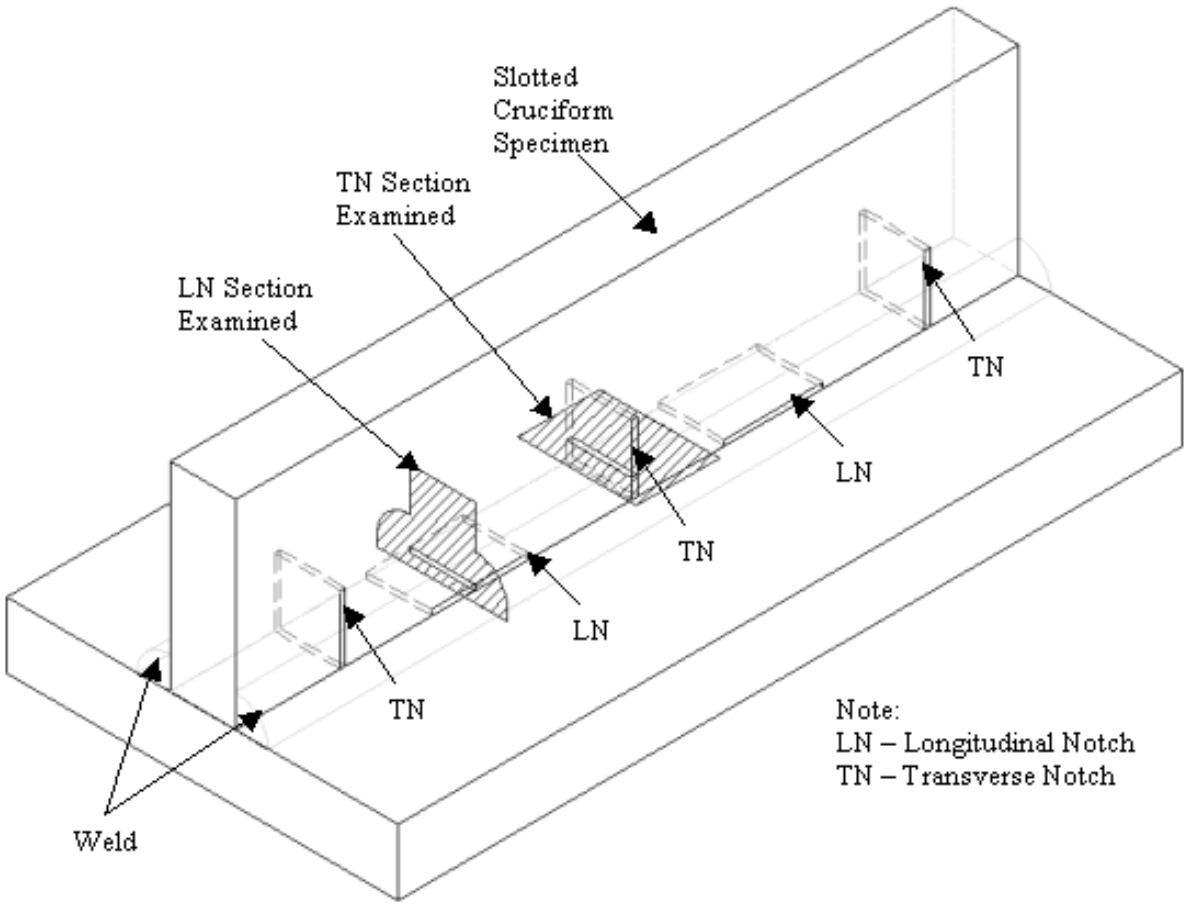


**Figure A3. Sectioning for the longitudinal and transverse notched areas**

**Figure 5A. Suggested data sheet for slotted cruciform test**

Company name _____ Date_____

Sheet____Of____

Job / test No._____

Description of Investigation_____

Base Metal Identification_____ Thickness_____

Base Metal Heat Treatment_____ Heat No._____

Composition:

C_____ Si_____ Mn_____ Si_____ S_____ Cr_____ Mo_____

Ni_____ V_____ Cu_____ Nb_____ Ca_____ B_____ Ti_____

Al_____ N_____

Welding Procedure Spec. No. _____Welding Process_____

Electrode/Wire Spec. No. _____Commercial Name_____

Diameter _____ Baking Treatment _____

Shielding Gas _____ Flow Rate _____

Shielding Flux_____Flux Size_____

Current _____ Preheat Temp. _____

Voltage _____Interpass Temp. _____

Polarity_____ Post-weld Heat Treatment_____

Travel Speed_____ Aging time _____

Heat input _____ Ambient Temp. _____

Test Weld Size _____ Ambient Humidity _____

Hydrogen Determination Method _____ Date _____

Diffusible Hydrogen Content _____

Actual Weld Pass Sequence

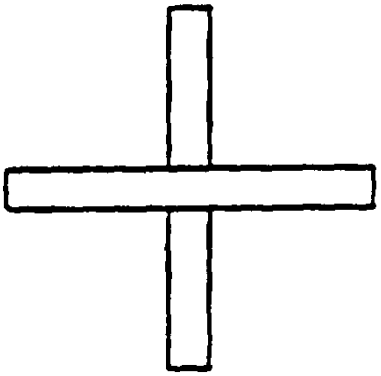

Results of Macrosection Examination:

| Quadrant / Section # | Type of Notch (L,T) | Crack Length Location | Quadrant / Section # | Type of Notch (L,T) | Crack Length Location |
|---|---|---|---|---|---|
| | | | | | |
| | | | | | |
| | | | | | |
| | | | | | |
| | | | | | |
| | | | | | |
| | | | | | |
| | | | | | |

Remarks_____

_____

Evaluated by _____ Date _____

Signature _____

## REFERENCES


1. Zapffee, C. A. and C. E. Sims, "Hydrogen Embrittlement, Internal Stress and Defects in Steel," *Trans AIME*, 145, 1941, p 225.
2. Petch, N. O. and P. Stables, "Delayed Fracture of Metals Under Static Load," *Nature*, 169, 1952, pg 842.
3. Troiano, A. R., "The Role of Hydrogen and Other Interstitials in the Mechanical Behavior of Metals," *Transactions of the American Society for Metals*, 52 (1), 1960, p 54.
4. Louthan, M. R., G. R. Ccaskey, J. A. Donovan, and D. E. Rawl, "Hydrogen Embrittlement of Metals," *Materials Science Engineering*, 10, 1972, p 257.
5. Beachem, C. D., "A New Model for Hydrogen Assisted Cracking," *Metallurgical Transactions* 3, 1972, p 357.
6. Structural Welding Code - Steel, ANSI / AWS D1.1-92, Appendix XI, Guide on Alternative Methods for Determining Preheat, 1992.
7. Matharu, I.S. and P.H.M. Hart, "Heat Affected Zone (HAZ) Cracking Behavior of Low Carbon Equivalent C-Mn Structural Steels," The Welding Institute Report No. 290/1985, November 1985.
8. Montemarano, T. W. et al, "High Strength Low Alloy Steels in Naval Ship Construction," *Journal of Ship Production*, Vol. 2, No. 3, August 1986, pp.145-162.
9. Kvidahl, L.G., "An Improved High Yield Strength Steel for Shipbuilding," *Welding Journal*, Vol. 64, No.7, July 1985, pp 42-48.
10. Czyryca, E. J., R. E. Link, R. J. Wong, D. A. Aylor, T. W. Montemarano, and J. P. Gudas, "Development and Certification of HSLA-100 Steel for Naval Ship Construction," *Naval Engineers Journal*, May 1990, pp 63-82.
11. Pellini, W. S., and C. E. Hartbower "Investigation of the Welding Factors Which Determine the Performance of Weldments," *Welding Journal, Welding Research Supplement*, October 1951, pp 499S-511S.
12. Satoh, K. and M. Toyoda, "Joint Strength of Heavy Plates With Lower Strength Weld Metal," *Welding Journal, Welding Research Supplement*, August 1975, pps 311S-319S.
13. NMAB: "Effective Use of Weld Metal Yield Strength for HY-Steels," National Materials Advisory Board, National Research Council, Report No. NMAB-380, January 1983.
14. Brenna, R.T, E.J. Czyryca, R.H. Juers, A.J. Wiggs, and R.J. Wong, "Review and Analysis of HY-130 Matching Yield Strength Weldments", DTRC/SME-88/79 May 1990.
15. Bridge Welding Code, ANSI/AASHTO/AWS D1.5-95.
16. NAVSEA Technical Publication T9074-AD-GIB-010/1688, "Requirements for Fabrication, Welding and Inspection of Submarine Structure", 1 May 1997
17. Ito, Y. And K. Bessyo, "Weldability Formula of High Strength Steels Related to Heat Affected Zone Cracking," IIW Document IX-576-68, 1968.
18. Yurioka, N., H. Suzuki, S. Oshita, and S. Saito, "Determination of Necessary Preheating Temperature in Steel Welding," *Welding Journal*, *Welding Research Supplement*, pp. 147S-153S, June 1983.

19. Yurioka, N., and T. Kasuya, "A Chart Method to Determine Necessary Preheat Temperature in Steel Welding," *Quarterly Journal of Japan Welding Society*, Vol. 13, No. 3, pp.347-357 1995.
20. Lazor, R.B., A. G. Glover, and B. A. Graville, "Properties and Problems in Structural Steel Welds," Welding Institute of Canada report, April 22, 1983.
21. Satoh, et. Al., (Working Group on restraint Intensity, Japan Welding Society/ Society of Naval Architects of Japan) "Japanese Studies on Structural Restraint Severity in Relation to Weld Cracking" (Preliminary Report), *Welding in the World*, Vol. 15 No. 7/8, 1977.
22. Cox, T.B. and A.H. Rosenstein, "A Review of Modern Naval Steels," Report # MATLAB 420, Naval Ship Research and Development Center, November 1969.
23. Potkay, G.P., "Microstructural Characterization of the Heat Affected Zone of HSLA-100 GMA-Weldment," Masters Thesis, Naval Postgraduate School, December 1987.
24. Lyttle, J.E., K.E. Dorschu, and W.A. Fragetta, "Some Metallurgical Characteristics of Tough High Strength Welds," *Welding Journal, Welding Research Supplement*, pp 493S – 498S, November 1969.

# SHIP STRUCTURE COMMITTEE PARTNERS AND LIAISON MEMBERS

## PARTNERS

**The Society of Naval Architects and Marine Engineers**

Mr. Joe Cuneo
President,
Society of Naval Architects and Marine Engineers

Dr. John Daidola
Chairman,
SNAME Technical & Research Steering Committee

**The Gulf Coast Region Maritime Technology Center**

Dr. John Crisp
Executive Director,
Gulf Coast Maritime Technology Center

Dr. Bill Vorus
Site Director,
Gulf Coast Maritime Technology Center

## LIAISON MEMBERS

American Iron and Steel Institute
American Society for Testing & Materials
American Society of Naval Engineers
American Welding Society
Bethlehem Steel Corporation
Canada Center for Minerals & Energy Technology
Colorado School of Mines
Edison Welding Institute
International Maritime Organization
International Ship and Offshore Structure Congress
INTERTANKO
Massachusetts Institute of Technology
Memorial University of Newfoundland
National Cargo Bureau
Office of Naval Research
Oil Companies International Maritime Forum
Tanker Structure Cooperative Forum
Technical University of Nova Scotia
United States Coast Guard Academy
United States Merchant Marine Academy
United States Naval Academy
University of British Columbia
University of California Berkeley
University of Houston - Composites Eng & Appl.
University of Maryland
University of Michigan
University of Waterloo
Virginia Polytechnic and State Institute
Webb Institute
Welding Research Council
Worchester Polytechnic Institute
World Maritime Consulting, INC

Mr. Alexander Wilson
Captain Charles Piersall (Ret.)
Captain Dennis K. Kruse (USN Ret.)
Mr. Richard Frank
Dr. Harold Reemsnyder
Dr. William R. Tyson
Dr. Stephen Liu
Mr. Dave Edmonds
Mr. Tom Allen
Dr. Alaa Mansour
Mr. Dragos Rauta
Mr. Dave Burke / Captain Chip McCord
Dr. M. R. Haddara
Captain Jim McNamara
Dr. Yapa Rajapaksie
Mr. Phillip Murphy
Mr. Rong Huang
Dr. C. Hsiung
Commander Kurt Colella
Dr. C. B. Kim
Dr. Ramswar Bhattacharyya
Dr. S. Calisal
Dr. Robert Bea
Dr. Jerry Williams
Dr. Bilal Ayyub
Dr. Michael Bernitsas
Dr. J. Roorda
Dr. Alan Brown
Dr. Kirsi Tikka
Dr. Martin Prager
Dr. Nick Dembsey
VADM Gene Henn, USCG Ret.

## RECENT SHIP STRUCTURE COMMITTEE PUBLICATIONS

Ship Structure Committee Publications on the Web - All reports from SSC 392 and forward are available to be downloaded from the Ship Structure Committee Web Site at URL:
http://www.shipstructure.org
SSC 391 and below are available on the SSC CD-ROM Library. Visit the National Technical Information Service (NTIS) Web Site for ordering information at URL:
http://www.ntis.gov/fcpc/cpn7833.htm

| SSC Report Number | Report Bibliography |
|---|---|
| SSC 430 | **Fracture Toughness of a Ship Structure** A.Dinovitzer, N. Pussegoda, 2003 |
| SSC 429 | **Rapid Stress Intensity Factor Solution Estimation for Ship Structures Applications** L. Blair Carroll, S. Tiku, A.S. Dinovitzer 2003 |
| SSC 428 | **In-Service Non-Destructive Evaluation of Fatigue and Fracture Properties for Ship Structure** S. Tiku 2003 |
| SSC 427 | **Life Expectancy Assessment of Ship Structures** A. Dinovitzer 2003 |
| SSC 426 | **Post Yield Stability of Framing** J. DesRochers, C. Pothier, E. Crocker 2003 |
| SSC 425 | **Fatigue Strength and Adequacy of Weld Repairs** R.J. Dexter, R.J. Fitzpatrick, D.L. St. Peters 2003 |
| SSC 424 | **Evaluation of Accidental Oil Spills from Bunker Tanks (Phase I)** T. McAllister, C. Rekart, K. Michel 2003 |
| SSC 423 | **Green Water Loading on Ship Deck Structures** M. Meinhold, D. Liut, K. Weems, T. Treakle, Woe-Min Lin 2003 |
| SSC 422 | **Modeling Structural Damage in Ship Collisions** Dr. A.J. Brown 2003 |
| SSC 421 | **Risk Informed Inspection of MarineVessels** Dr. B.M. Ayyub, U.O. Akpan, P.A. Rushton, T.S. Koko, J. Ross, J. Lua 2003 |
| SSC 420 | **Failure Definition for Structural Reliability Assessment** Dr. B. M. Ayyub, P.E. Hess III, D.E. Knight 2002 |
| SSC 419 | **Supplemental Commercial Design Guidance for Fatigue** R.A. Sielski, J. R. Wilkins, J.A. Hultz 2001 |
| SSC 418 | **Compensation for Openings in Primary Ship Structure** J.J. Hopkinson, M. Gupta, P. Sefcsik 2002 |